Dear Professor **Yevgeny Aksenov and the Reviewers**

Revision of TC manuscript tc-2020-44:

Sea Ice Drift and Arch Formation in the Robeson Channel Using Daily Coverage of Sentinel-1 SAR Data During the 2016–2017 Freezing Season

We would like to thank the reviewers for taking time to review the manuscript and offering suggestions to improve the manuscript. We have revised our paper according to the reviewers' comments, which are summarized in the following. We also made major changes to improve the flow of the information and reduce the size of the text.

(1) According to the comments of **Reviewer 1**, we obtained regular data of the ocean currents and addressed the separation of the contributions of wind and ocean currents to the ice drift and reported in Section 4.3.1 using a statistical approach. In addition, we studied the tidal effect on ice motion in the Robeson Channel extensively. Tidal effect could be assumed to have much smaller influence on ice drift in the Robeson Channel than the other regimes in Nares Strait according to Johnson et al. (2011). Meanwhile, we could not conclude from ice drift velocity records from IABP buoys how tide impacted ice drift in the Robeson Channel. This conclusion was reached after we calculate the Fourier spectra of the velocity record from each buoy and found no persistent peaks from data of 9 buoys.

(2) According to the comments of **Reviewer 2**, we clarified the motivation and contribution of this study, and the advantage of using manual tracking of individual sea ice floes as opposed to generating gridded ice motion vectors. More statements were added in the manuscript. Although we studied two approaches about the tide effect in the Robeson Channel, we could not duplicate this work in our study because of limitations that have been clarified in the following response letter.

For more details, please refer to the two response letters attached below. In addition, the we corrected many mistakes in the language of the manuscript, then we use service from a professional English language editor from the Member Chartered Institute of Editing and Proofreading. We hope that you are satisfied with the revised version. Thanks once again for your time.

Best Regards,

The authors

Response to Reviewer 1

In the following we include the reviewer's comments and our response, item-by-item. RC refers to reviewer's comment.

RC: The paper analyzes ice floe movement with SAR satellite data in Robeson Channel during the 2016-2017 freezing season. Individual floes are tracked using daily images and conclusions are drawn on the transport of ice with respect to wind, ice congestion and current. The paper is unable to separate the contributions of wind and current, while no mention is made of tidal affects.

Response: We clarified the approach of the study in the opening of Section 4.3.1 in the revised version. We confirm that we mainly studied the impact of wind on ice floe motion but we also consider impacts of four other sources; ocean currents, tide (both in the Robeson Channel) and the sea surface height (SSH) at the wider scale of the Lincoln Sea. Those factors are considered only when wind does not explain the observed ice drift. This information provides the basis for the discussions of ice floe drift north and within the Robeson Channel in the two separate parts in the same section. This point is also added to the objective of the study at the end of the Introduction.

Thanks for your suggestion, we obtained regular data of the ocean currents and addressed the separation of the contributions of wind and currents to the ice drift in Section 4.3.1 using a statistical approach. However, we believe that separation of these two influences can better be achieved through a modelling approach as mentioned in the second paragraph in the sub-section titled "*ice drift within the Robeson Channel*" in 4.1.3.

As for the tidal effect in ice floe motion we expanded our study to cover this point. Explanation of what we did is included in our response to Specific Comments Line 46 below.

RC: The paper also documents the formation of an ice arch in the vicinity of Robeson Channel during the 2016-2017 season. No historical context of this event is given.

Response: Thanks for the comment. We chose 2016/2017 dataset because it was available from Sentinel-1. The mechanism of the arch development in this year must be typical of the other years. No historical context of the ice arch was given because we thought it was outside the scope of the study. For the ice arch, the objective of the study is to monitor the development of the arch's shape using the daily SAR data. We believe that the information is new because no daily SAR data were available for this region before the S1 constellation. In fact, this daily coverage was the motivation behind the study. As the reviewer pointed out, previous studies addressed the interannual variability of the arch's locations. We did not cover this information but we are showing, for the first time as far as we know, the daily development of the arch's shape until it stabilized and the role of the wind on altering the shape. We included three

references that address the historical context of the arch in Nares Strait in the first paragraph of Section 4.2.

RC: The paper has an overabundance of parenthetical statements and some poor wording.

Response: Thanks for your suggestion. We removed many parenthetical statements. We also corrected some wrong and poor sentences. The language of this manuscript was improved by a professional editor named Mark Ackerley from Member Chartered Institute of Editing and Proofreading.

Specific Comments

RC:46: No mention of tides. The strongest tides in the Canadian Arctic are in Kane Basin to the south. Tides can reverse the strong surface current in Smith Sound on a diurnal basis. What are the tidal effects in Robeson Channel?

Response: We checked the tide data in this region and found very few sets, mostly capitalized on opportunities of expeditions for other purposes. For example, Münchow et al., (2007) and Münchow and Melling (2008) measured ocean currents in the Nares Strait using mooring buoys, most of which were located at the southern end of Kennedy Channel. They found that tides impacted the dominant component of current in Nares Strait (as the reviewer mentioned). However, Münchow et al. (2007) indicated that the amplitudes and phases of tidal constituents varied substantially both along and across the strait. Meanwhile, Johnson et al. (2011) indicated that Petermann Fjord, at 81°N, is well above the critical latitude for the M2 tide (74.5°N). Since the Robeson Channel is above the latitude of Petermann Fjord, therefore, tidal effect is assumed to have much smaller influence on ice drift in the Robeson Channel than the other regimes in Nares Strait.

Gimbert et al. (2012) used Fourier spectra of the buoy velocity from the International Arctic Buoy Program (IABP) to discuss the impact of tidal effect in the Arctic basin. We checked all available buoy datasets and found 9 buoys operated through the Nares Strait during September-April from 1979 to 2016. We calculated the Fourier spectra of the velocity record from each buoy. Figure 1 is an example from 2 buoys.

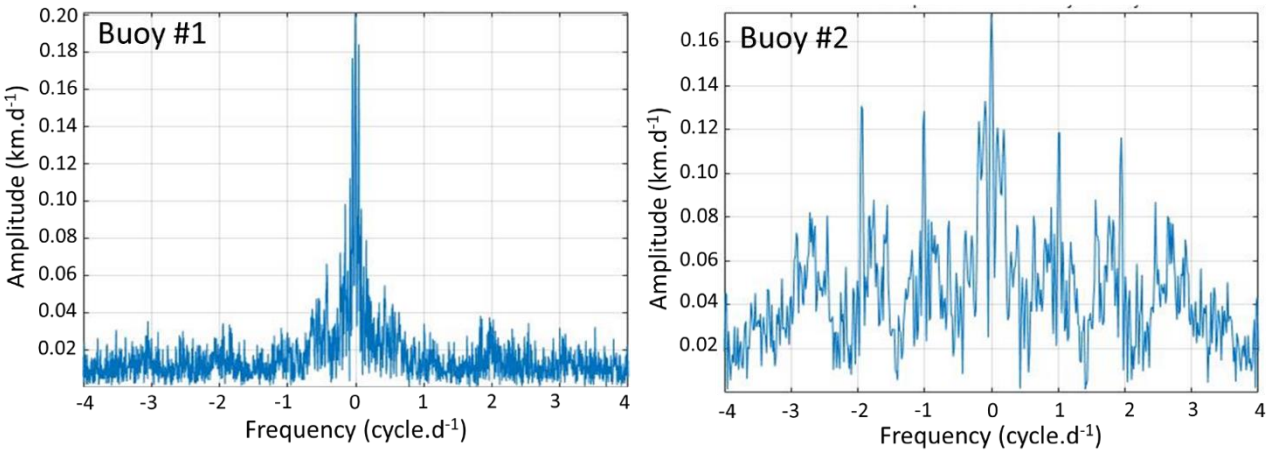

Figure 1. the Fourier spectra of the velocity record from two buoys.

The spectra of motion from the 9 buoys are different, some with identifiable peaks and others with no peaks. Peaks may be linked to the regular frequency of the tide. So, we could not conclude from these data how tide impacted ice drift in the Robeson Channel. A few statements are added in the manuscript, from Line 269 to 282 to explain this point. Please see third paragraph in Section 4.1.3

Münchow and Falkne (2006) addressed two independent methods to estimate tidal currents. The first is a numerical model of barotropic tidal currents that predicts depth-averaged tidal currents on a 5-km horizontal grid. The second relied upon the method of least squares to minimize residual tidal variance in the data. However, we could not duplicate this work in our study because of two limitations; the first is the coarse resolution of the numerical model that is not consistent with spatial resolution of ice floes data in our study. The second is no horizontal gradients of tidal properties within the limited study area which has to be used in the Least Squares method. Therefore, we will focus on how to resolve tidal effect from sea ice velocity from high spatial resolution satellite images in a future study (please note that these statement are not included in the manuscript).

Münchow, A., Falkner, K. K., and Melling, H.: Spatial continuity of measured seawater and tracer fluxes through Nares Strait, a dynamically wide channel bordering the Canadian Archipelago, Journal of Marine Research, 65(6): 759-788, 2007.

Münchow, A. and Melling, H.. Ocean current observations from Nares Strait to the west of Greenland: Interannual to tidal variability and forcing, Journal of Marine Research, 66(6): 2008, 801-833.

Johnson, H. L., Münchow, A., Falkner, K. K., and Melling, H.: Ocean circulation and properties in Petermann Fjord, Greenland, J. Geophys. Res., 116, C01003, doi:10.1029/2010JC006519, 2011.

Gimbert, F., Marsan, D., Weiss, J., Jourdain, N. C., and Barnier, B.: Sea ice inertial oscillations in the Arctic Basin, Cryosphere, 6, 1187–1201, 2012.

Münchow, A. and Falkner, K. K.: An Observational Estimate of Volume and Freshwater Flux Leaving the Arctic Ocean through Nares Strait, Journal of Physical Oceanography, DOI: 10.1175/JPO2962.1, 2006.

RC: 56: An ice tracking algorithm using short-time span AVHRR imagery was developed in Nares Strait in 2000. doi.org/10.1080/07055900.2001.9649681

Response: We checked this paper and referred to it in the Introduction (in Line 61 in the revised manuscript). It included a limited data set from AVHRR between March and August 1998. The ice tracking was performed using the commonly-used method of maximum cross-correlation. While the temporal resolution was fine-enough (5 hours) the spatial resolution was poor (from AVHRR). Our manuscript generates drift of individual ice floes, which can only be obtained from the fine-resolution SAR data when it become available daily. Thanks to the Copernicus program that made the S1 SAR constellation data accessible for free.

RC: 70: Kwok is referring to the absence of both the North Water polynya ice arch to south and the northern ice arch in the vicinity of Robeson Channel. The northern ice arch featured in this paper has occurred 17 times since 1979, and on four occasions it was the only ice arch in the Nares Strait system. The location of the northern ice arch is highly variable. In 2007 there were no ice arches. Normally, the northern ice arch forms first followed by the southern ice arch, at which point Nares Strait becomes solid ice. This paper does not put the ice arch into a historical context. doi.org/10.1038/s41598-019-56780-6

Response: Thanks for this information which briefly highlights a historical context of the arch. We have included it in the opening of Section 4.2 (Line 463 in the revised manuscript). As mentioned above, the objective of the arch section in this manuscript is monitoring its development on daily basis, starting from the onset of formation until it stabilized. We believe that this information applies to any arch at any location in the Nares Strait system.

RC: 84: What is the re-visit time for RCM? Once per day is poor temporal resolution for ice tracking in this regime.

Response: There is no fixed temporal resolution (i.e. re-visit time) of any SAR system at any given location because the senor is not open for data acquisition throughout the entire orbit. It is open only for about 28 minutes or so in each orbit of about 100 minutes. Hence, the frequency of the coverage should be requested by the user and approved by the acquisition plan of the satellite. We were lucky to have the daily coverage of this area from S1 constellation (S1-A/B). The advantage of such frequent coverage, as demonstrated in this study, can be used to support daily acquisition of SAR from RCM in critical areas in the future. In a relevant study, Lange et al. (2019) also used airborne observations to backtrack sea ice floes and calculated the drift speed. According to Table 1 in this research, the minimum time interval is 3 days, and the maximum time interval is 10 days. The temporal resolution in our study was better (1 day).

Lange, B. A., Beckers, J. F., Casey, J. A., and Haas, C.: Airborne observations of summer thinning of multiyear sea ice originating from the Lincoln Sea. Journal of Geophysical Research: Oceans, 124. https://doi.org/10.1029/2018JC014383, 2019.

RC: 124: No units for the x-axis for Figure 2

Response: The unit for all segments is the same as the unit attached to the bottom segments (km h^{-1}). This is now mentioned in the caption.

RC: 154: How likely is it that the floe travels in a consistent straight line over a 24-hour period?

Response: It depends primarily on the varying wind direction and the geometry and mechanical properties of the surrounding floes. A statement to confirm this point is added in Section 3, Line 177 in the revised manuscript. However, there are no quantitative results due to the limited in-situ data.

We checked all available buoy datasets in the Arctic, and found that 12 buoys from IABP during the period from 1979 to 2016 drifted through the Nares Strait. We chose 9 buoys out of the 12 buoys consistent with our study period (September to the next April). The temporal resolution of the buoys data is 3 hours. We used the geographical coordinates of the first temporal point in two successive days from each buoy to calculate the drifting distance and call it simulated daily distance. Then, we summed the distances during the rest of the 3-hours interval in each day, and compared them to simulated daily distances. The R^2 is 0.945, which indicates close relationship between simulated daily distances and 3-hours-sum distances. Therefore, the assumption of a linear path of the floe between two successive days is reliable to be employed under the limited temporal resolution of Sentinel-1A/1B. The following graphs show results from this test. In order not to increase the size of the manuscript and the number of figures, we did not include the description and results from this test.

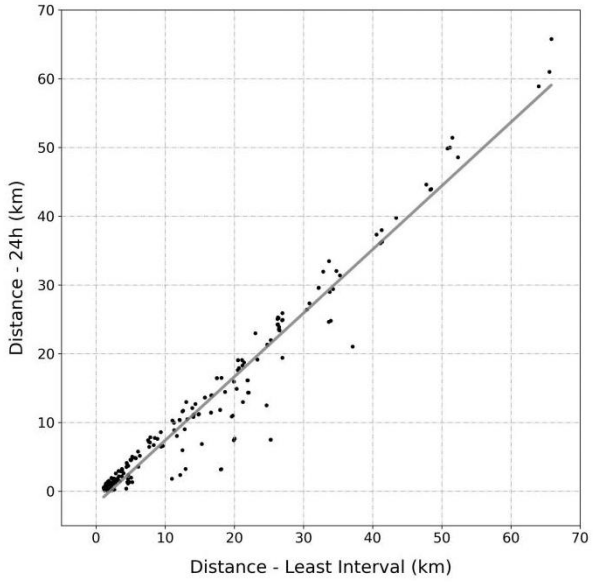

Figure 2. Difference between 24h interval distance and 3h interval distance.

In Fig. 2, “Distance-Least interval” is from 3h IABP data, “Distance-24h” is daily data using two records from two successive days. The difference is large if daily displacement is big.

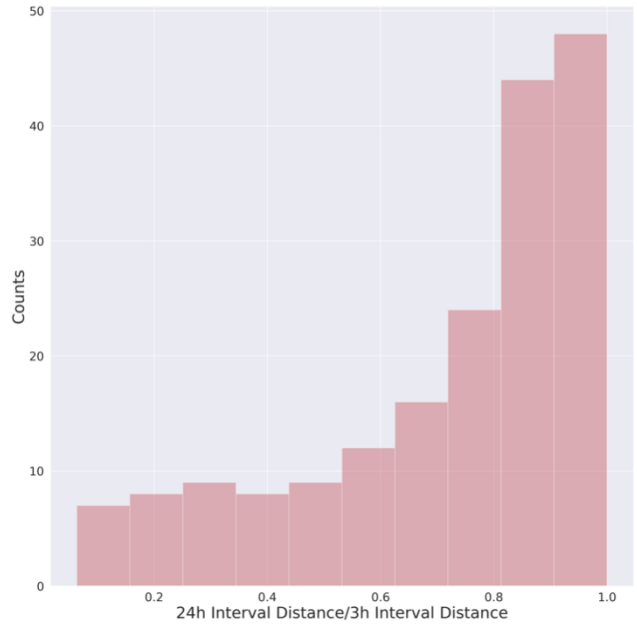

Figure 3. 24h interval distance/ 3h interval distance and corresponding counts.

In Fig. 3, X-axis is 24h displacement (daily data using two records from two successive days), i.e. sum of 3h displacement (8 records in one day). Y-axis is the corresponding counts. This figure indicates that most 24h displacement is similar to sum of 3h displacement. But there is no significance after calculating T-mean.

RC: 186-200: Very confusing. 16 floes are mentioned, then 39 floes, while the figure mentions16 floes and shows 31 floes.

Response: Thanks for this comment. Yes, it was indeed confusing. We examined 39 floes and numbered them #1, #2, …, #39. The order has no significance. In Fig. 4 we show tracks of 16 floes out of the 39 (we deleted 4 of them in the new manuscript so there are 12 floes in Fig. 4 now) and we attach the floe numbers. It just happened that the 12 floes we selected are numbered 1, 2, 3, 4, 5, 20, 21, 23, 24, 26, 29, and 31. All these floes remain long enough in the channel, so the motion tracking reveal different features that are addressed in this section. The statements in Section 4.1.1 was modified to include the above explanation, starting from Line 209 in the revised manuscript.

RC: 250: Can any useful conclusion be derived from the SSH map? Why is the December 2016 average shown?

Response: As mentioned in the text, the SHH maps, obtained as weakly, show a gradient that contributes to the large-scale motion of the entire ice cover north of the Robeson Channel. SSH map presented in the manuscript, averaged over December 2016 from GLORYS12V1, is just an example. It is in the middle of the study period. We list all monthly SSH maps in the following figure (not included in the manuscript).

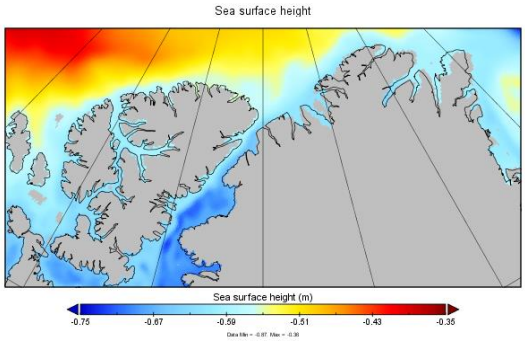

September, 2016

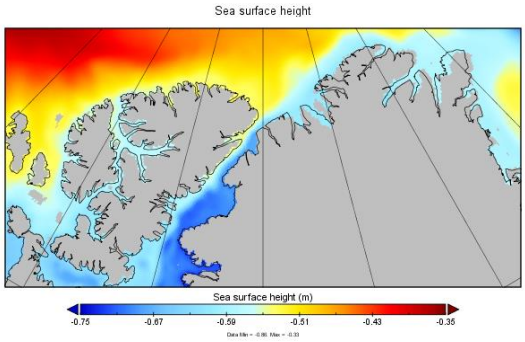

October, 2016

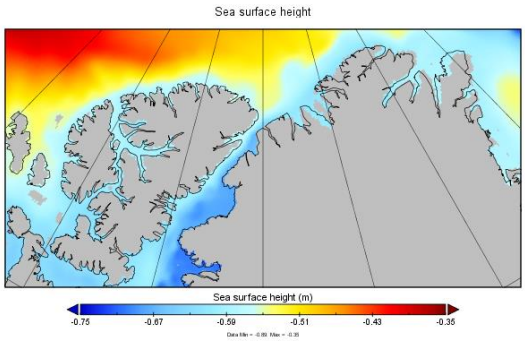

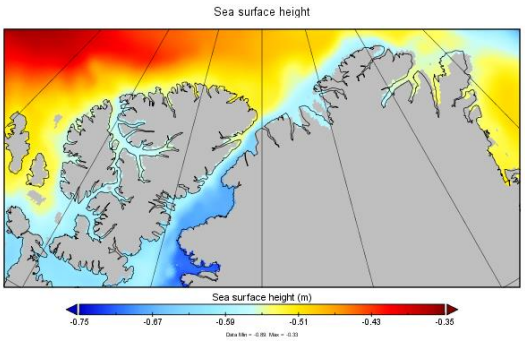

November, 2016 December, 2016

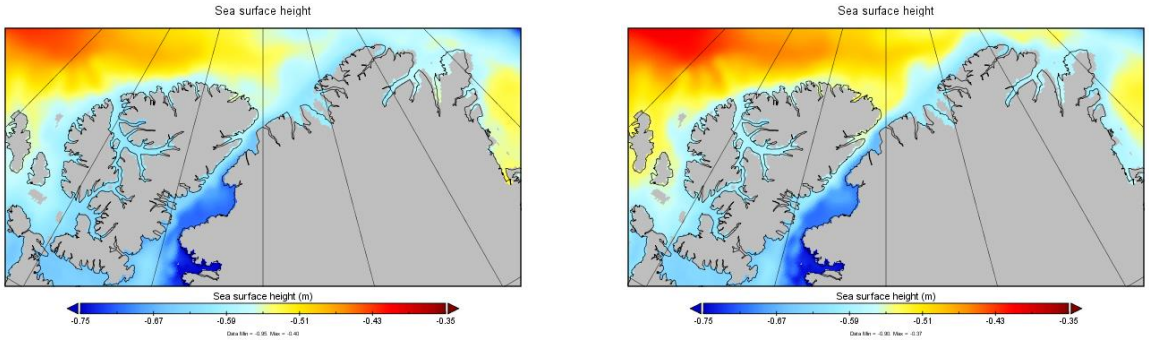

January, 2017 February, 2017

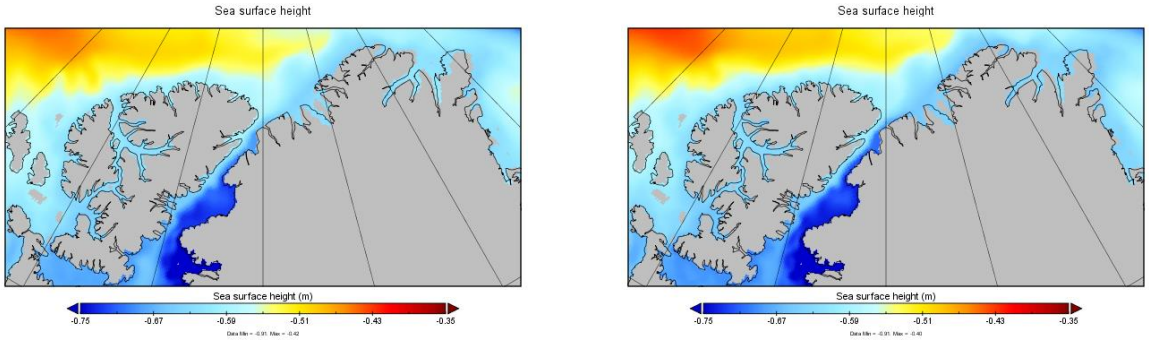

March, 2017 April, 2017

Figure 4. Monthly SSH maps from September 2016 to April 2017.

RC: 295: The description of the wind vectors in the caption is incomprehensible.

Response: We believe the reviewer was referring to the caption of Fig.9. We modified this caption to make it comprehensible (Line 343 in the revised manuscript). Captions of similar figures were also modified. Here we repeat that in each panel of the wind data, the colors indicate the wind vectors that were available at 3-h interval between the 2 acquisition times of the satellite in the two successive days shown in the label.

RC: 376: Why were these floes moving so fast?

Response: Because these 2 floes originated in the polynya after the arch formation. So, they were not surrounded by ice floes that impact their motion. They move within water and thin ice. This point is mentioned in the beginning of the section titled "*Ice drift within the Robeson Channel"* from Line 351 to Line 355 in the revised manuscript.

RC: 379: Are the authors suggesting the SSH gradient is the reason for the movement? Is there a reference for this?

Response: Yes. Wekerle et al. (2013) mentioned that the SSH difference between the Arctic Ocean and Baffin Bay (Figure 7b in the following paper) not only leads to a net outflow from the Arctic Ocean, its variability also drives the variation of the CAA throughflow. We added this reference in the revised manuscript in Line 302.

Wekerle, C., Wang,Q., Danilov, S., Jung, T., and Schröter, J.: The Canadian Arctic Archipelago throughflow in a multiresolution global model: Model assessment and the driving mechanism of interannual variability, J. Geophys. Res. Oceans, 118, 4525–4541, doi:10.1002/jgrc.20330, 2013.

RC: 380: First sentence makes no sense. What is 'it' and what other effects did 'it' overcome?

Response: Thanks for your comment. Yes, the sentence was not clearly phrased. Now it reads "Between 16 and 18 November, the same strong wind, which approached 30 km h^{-1}, continued to blow to the northeast (Fig. 13), and the entire set of floes responded by drifting in the same direction" in Line 418 in the revised manuscript.

RC: 381: Why are the floes moving northeast under light winds from the south? Tide?

Response: Between 15 and 16 November wind between 20 and 37 km h^{-1} blew from the south but the floe moved eastward. As we mentioned before, we could not confirm the role of the tide but the slope of SHH (west-east) is mentioned as a possible explanation. Between 16-18 November the entire set of ice floes moves in same direction of the wind. Between 18 and 19 November the wind virtually diminished, but a group of floes appeared to swirl clockwise. We checked the current data from 15 to 19 November and found it did not explain the motion. Therefore, we postulate that a combination of current and internal forces between floes determine the motion in absence of wind effect. This is now mentioned at the end of Case study 2, starting from Line 415 in the revised manuscript. This is a case where it is difficult to confirm the drive for the motion from the present data.

RC: 395: How is land fast ice different from sea ice with respect to physical properties. Would this change the drift rate?

Response: Landfast ice is not different than mobile ice in most of physical properties (e.g. salinity, density, dielectric and thermal properties, etc.). However, its crystalline structure may feature larger crystals with larger brine spacing. But this does not affect the radar signature. What makes a difference in the radar signature (and the physical appearance of the ice) is the surface roughness, which is not a physical property by the way. Mobile ice is usually rough and landfast ice is usually smooth, except at its edge. Hence, landfast ice usually has low

backscatter. As for the ice floe drift, a floe would slow down as it passes along the edge fast ice because of the shear action.

As for tracking the motion of floe #38, which we think has raised the question by reviewer, the drift is not affected by the origin of the floe but rather by the moderate concentration of the ice that surround the floe in addition to the wind/current combination. This is what Case Study 3 is showing. relates the drift to the wind speed and direction. The floe drifted in an open drift ice regime.

RC: 425: Reference for Antarctic polynya statement?

Response: Thanks for your suggestion. We added the paper by Nihashi et al. (2015) in Line 463 in the revised manuscript. In Nihashi et al. (2015), a map of all polynyas in the Antarctic region was presented. All are coastal polynyas.

RC: 426: As stated earlier, there is no context given for the ice arch formation.

Response: We included a brief context that starts with the sentence "In the case of the Robeson Channel, an ice arch commonly forms at the inlet of the channel, ….." in Line 463 in the revised manuscript. We added 3 references to help interested readers to obtain further historical context of this ice arch. This comes after the line the reviewer referred to.

Technical Corrections

RC: 35: existing?

Response: We changed the word to "presence" in Line 36 in the revised manuscript. Thanks for drawing our attention to this error.

RC: 176-177: Poorly written sentence.

Response: Yes, it was poorly written. The whole paragraph has been rewritten, now it reads "The ice floe motion is considered in two separate regimes: north of the Robeson Channel near its entrance and within the Robeson Channel….", starting from Line 197 in the revised manuscript.

RC: 187: '39' not 'thirty-nine'

Response: Thanks for your suggestion. We follow the requirement of TC:

- **Numbers**
  - For items other than units of time or measure, use words for cardinal numbers less than 10; use numerals for 10 and above (e.g. three flasks, seven trees, 6 m, 9 d, 10 desks).

We use words less than 10, use numerals for 10 and above. All the numbers in the manuscript has been checked and modified now.

RC: 194: 'Remarkably' has no scientific meaning. Quantify.

Response: Thanks for your suggestion. We quantified it "by a factor of 1.5–5" in Line 217 in the revised manuscript. This range is obtained from Fig. 5.

RC: 246: 'that' not 'which'

Response: The sentence's structure has been modified in Line 297 in the revised manuscript. Thanks.

RC: 260: 'path' not 'bath'

Response: It was corrected in Line 312 in the revised manuscript. Thanks.

RC: 270: Should not give directions for explanations. It is done quite often in the paper.

Response: Removed part of the explanation in Line 316 in the revised manuscript.

RC: 274-280: I lost count of how many parenthetical statements are in this paper. It really hinders the flow of the narrative.

Response: Thanks for your suggestion. We eliminated many of those parenthetical statements to make the reading flows better.

RC: 300: Table 2 has a speed in 'km'. Per day?

Response: Yes, km d^{-1}. It is now corrected in Table 2 in the revised manuscript.

RC: 324: Be consistent with wind direction. Northerly wind or southward blowing. The terms vary throughout the paper. Not sure why northerly is defined here.

Response: Northerly, southerly, northwesterly, etc. are consistent with meteorological jargon. It is shorter in writing. We changed the term to northward blowing, southward blowing, northeastward, etc.

RC: 342: Do not use 'i.e.' in the narrative.

Response: We removed "i.e." and adjusted the sentence in Line 371 in the revised manuscript.

RC: 380: Why is 'continues' in present tense?

Response: It was changed to the past tense and modified the sentence starting from Line 420 in the revised manuscript.

RC: 400: Three times 'remarkably' has been used the paper.

Response: The word "remarkably" was removed in the revised manuscript.

RC: 419: 'polynyas' Also, do not tell the reader what is well known.

Response: 'Polynyas' is corrected. Yes, indeed we are telling the reader what is well known in one sentence that addresses the two mechanisms of polynya formation (citing the original reference of Smith at el. (1990)). The reason for this is to introduce the following sentences that are telling the reader what is not well-know; namely a necessary, though not sufficient, condition for polynya formation. That is the formation of an ice arch. This is necessary in order to block a possible stream of ice drift from a nearby source as in the case of the present area, namely the ice coming from the Lincoln Sea. This ice continues to flow to fill the location where the physical conditions for the polynya formation are indeed satisfied. Without the arch, there will be no typical polynya of considerable amount of open water and thin ice even if the conditions of polynya mechanisms are satisfied. We did not find this information in the literature and we would appreciate it if someone could point it out a reference in a previous publication so we can use it.

We deleted 'It is well known that' in Line 458 in the revised manuscript.

RC: 482: 'chopping' is a poor term

Response: 'chopping' is replaced by "detachment of ice pieces" in Line 518 in the revised manuscript.

Response to Reviewer 2

In the following we include the reviewer's comments and our response, item-by-item. RC refers to reviewer's comment.

RC: This study investigates the formation structure of the ice arch at the north end of Nares Strait and sea ice floe drift characteristics in Robeson Channel (RC) using a time series of sequential S1-A/B SAR images. While the presentation quality of the figures is generally quite good, I find that the analysis is mostly descriptive and qualitative and as such only really documents some observations and prepares some statistics as opposed to generating any new scientific information on the processes and their relative importance/contribution in comparison to previous studies or the larger sea ice environment of the region.

Response: The study generates information and statistics of ice drift in the narrow water passage of the Robeson Channel. During the course of this study we found that most tracking methods cannot retrieve ice drift in narrow straits. And even when they cover the larger ice cover. they do not retrieve the motion of individual ice floes. Motion of hazard ice floe is an operational requirement, which yet to be developed. The daily SAR images is the only tool to achieve this purpose. The present study demonstrated this potential. Recent and future SAR constellation systems are geared towards fulfilling this requirement. Sentinel-1 system has been the first one.

An examples of ice motion vectors from an operational product is presented in the following figure using a commonly-used feature tracking method. As can be seen, most retrieved vectors are located in the Lincoln Sea with virtually no vectors in the Robeson Channel.

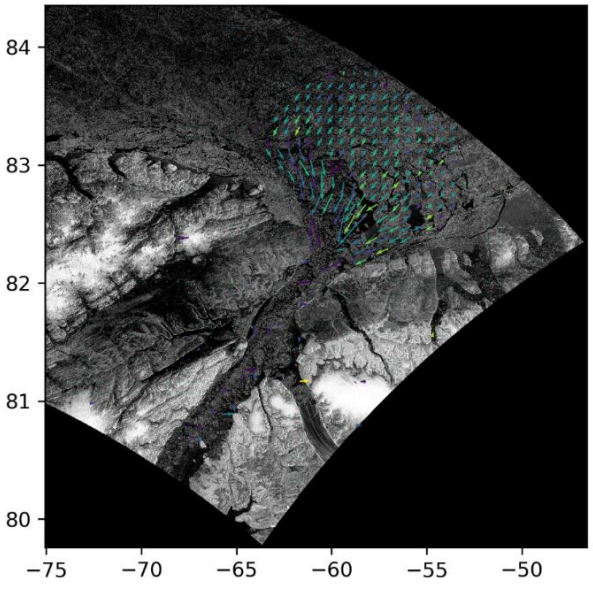

We acknowledged the availability of S1 data from the Copernicus program at no cost, which facilitated this study.

As the focus of this study is on motion of individual ice floes (not the overall ice cover), comparison to previous studies was not included because those studies focus on ice motion in the Nares Strait, with particular attention on Kennedy Channel and Kane basin. In our view, the new scientific information presented in the manuscript is about the motion of individual floes and the relative contribution of the wind and ocean current when floes are drifted in open drift regime (low ice concentration). We demonstrate that when ice floes are surrounded by high concentration the contributions of these two factors are reduced. Also, we think the information about development of the ice arch, as triggered by wind, is new and was made possible only using the daily SAR coverage.

Information from the study can be used to verify ice drift products from coarse-resolution products (the finest is at 0.083°). We are currently assessing four sea ice motion products in the RC using daily Sentinel-1 images from September 2016 to August 2017.

Admittedly, the process of estimating the drift vectors in this study starts with manual tracking of several ice floes in sequential images. While this is a subjective and laborious task, we believe it is most accurate. This is now mentioned in the last paragraph of the Introduction with more justification of the objective of the study. The analysis includes qualitative descriptions and quantitative data. In this revised version we added more quantitative analysis by combining wind and ocean current data in a multivariate analysis to asses the relative weight of each factor on floe motion (we downloaded daily gridded ocean current data in the Robeson Channel). With this statistical approach we found that wind and ocean current explain 72.9% and 16.5% of the floe motion, respectively.

We would like to assert that this study is mainly about identifying links between ice floe motion and the wind field. That is because we have regular gridded reanalysis wind data. When wind does not explain the ice floe motion, we explore other factors starting with ocean current (daily gridded data also available). This is now mentioned in the last paragraph of the Introduction. We qualify the wind contribution as “significant” when we find that floe motion follows wind direction with speed proportional to wind speed. Results show that wind contribution is important when floe moves within low ice concentration or when the surrounded ice cover constitutes thin ice (as in the case of the polynya after the arch formation).

RC: I also strongly agree with Reviewer#1 in that the tidal influence on ice floe movement is largely ignored, thus generating considerable uncertainty in the relative contribution of the other factors cited as being significant (i.e. wind speed, ocean current estimates, ice consolidation/concentration, etc.).

Response:

We though that if the tide frequency is twice per day it will not be captured by the daily data from Sentinel-1. In this revision we expanded our study to cover tidal forcing. We checked the tide data in this region and found very few sets, mostly capitalized on opportunities of expeditions for other purposes. For example, Münchow et al., (2007) and Münchow and Melling, (2008) measured ocean currents in the Nares Strait using mooring buoys, most of which were located at the southern end of Kennedy Channel. They found that tides impacted the dominant component of current in the Nares Strait. However, Münchow et al. (2007) indicated that the amplitudes and phases of tidal constituents varied substantially both along and across the strait. Meanwhile, Johnson et al. (2011) indicated that Petermann Fjord, at 81°N, is well above the critical latitude for the M2 tide (74.5°N). Since the Robeson Channel is above the latitude of Petermann Fjord, therefore, tidal effect is assumed to have much smaller influence on ice drift in the Robeson Channel than the other regimes in Nares Strait.

Gimbert et al. (2012) used Fourier spectraof the buoy velocity from the International Arctic Buoy Program (IABP) to discuss the impact of tidal effect in the Arctic basin. We checked all available buoy datasets and found 9 buoys operated through the Nares Strait during September-April from 1979 to 2016. We calculated the Fourier spectraof the velocity record from each buoy. Here is an example from 2 buoys.

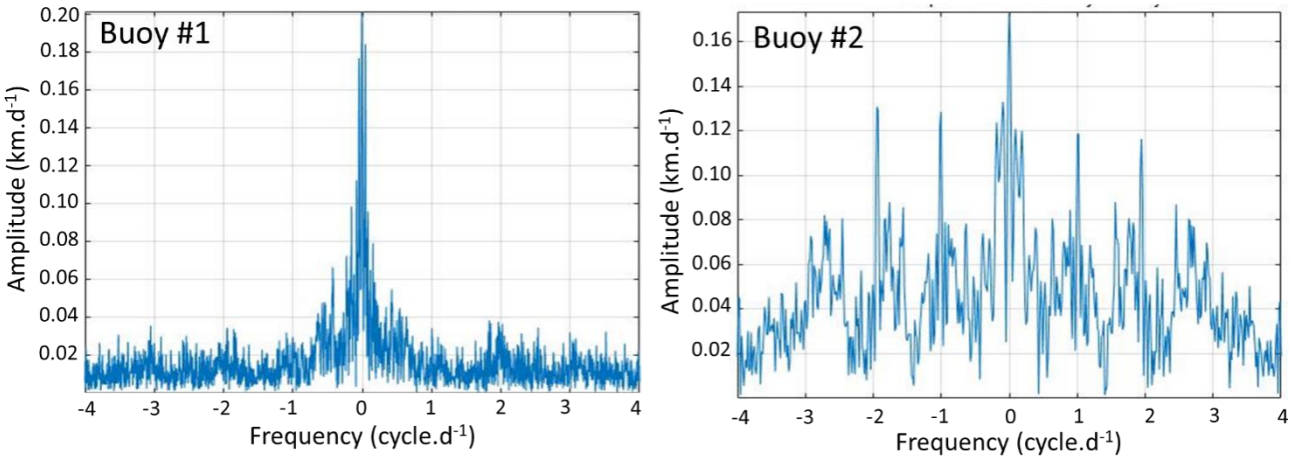

The spectra of motion from the 9 buoys are different, some with identifiable peaks and others with no peaks. Peaks may be linked to the regular frequency of the tide. So, we could not conclude from these data how tide impacted ice drift in the Robeson Channel. The discussion is added in the revised manuscript, from Line 269 to 282.

Münchow and Falkne (2006) addressed two independent methods to estimate tidal currents. The first is a numerical model of barotropic tidal currents that predicts depth-averaged tidal currents on a 5-km horizontal grid. The second relied upon the method of least squares to minimize residual tidal variance in the data. However, we could not duplicate this work in our study because of two limitations; the first is the coarse resolution of the numerical model that is not consistent with spatial resolution of ice floes data in our study. The second is no

horizontal gradients of tidal properties within the limited study area which has to be used in the Least Squares method. Therefore, we plan to focus on how to resolve tidal effect from sea ice velocity from high spatial resolution satellite images in a future study.

Münchow, A., Falkner, K. K., and Melling, H.: Spatial continuity of measured seawater and tracer fluxes through Nares Strait, a dynamically wide channel bordering the Canadian Archipelago, Journal of Marine Research, 65(6): 759-788, 2007.

Münchow, A. and Melling, H.. Ocean current observations from Nares Strait to the west of Greenland: Interannual to tidal variability and forcing, Journal of Marine Research, 66(6): 2008, 801-833.

Johnson, H. L., Münchow, A., Falkner, K. K., and Melling, H.: Ocean circulation and properties in Petermann Fjord, Greenland, J. Geophys. Res., 116, C01003, doi:10.1029/2010JC006519, 2011.

Gimbert, F., Marsan, D., Weiss, J., Jourdain, N. C., and Barnier, B.: Sea ice inertial oscillations in the Arctic Basin, Cryosphere, 6, 1187–1201, 2012.

Münchow, A. and Falkner, K. K.: An Observational Estimate of Volume and Freshwater Flux Leaving the Arctic Ocean through Nares Strait, Journal of Physical Oceanography, DOI: 10.1175/JPO2962.1, 2006.

RC: I also found the manuscript to be overly long with perhaps 3-5 too many figures. Multiple grammatical issues (listed below) made for an onerous read. While the research is likely publishable somewhere, I feel that the manuscript might be better suited for another journal, perhaps Remote Sensing, since it largely fails to generate any new process understanding.

Response: Thanks for the comment. We downloaded some papers from TC and manuscripts from TCD and found that our manuscript is not overly long. Perhaps papers from TC look shorter because they are presented in double column. However, considering the reviewer's suggestion, we have reduced the text and deleted Fig. 11 and the relevant text. We removed 4 panels from Fig. 4 (floes #7, #8, #12 and #30). As for grammatical mistakes, we corrected what the reviewers pointed to, checked and corrected other mistakes, and finally sent the manuscript to a professional editor to help us polish the language.

We would like to suggest that the manuscript enhances understanding of two processes. The first is about the influence of wind and ocean current on drift of individual floes in relation to the ice concentration that surrounds the floe track. The high concentration with the momentum of surrounding floes overrides possible effect of any other factor. Secondly is the monitoring the ice arch formation. This information cannot be obtained from any satellite observations other than daily SAR data, which was used here for the first time.

Of course, we could have submitted this manuscript to any journal on remote sensing for ice application but we chose The Cryosphere because it is a Copernicus publication and Sentinel-1 is a Copernicus initiative through which the data used in this study were made available.

Minor Comments

RC: L5 – 'Meteorological' is spelled incorrectly

Response: The spelling mistake has been corrected to 'Meteorological' in Line 5 in the revised manuscript.

RC: L29 – You say RC is about 80km in length, but your scale bar and associated 'box' indicating RC in Fig 1 suggests that RC is more on the order of 150 km long. Either the 'box' in Fig 1 must be shortened or adjust the length in the text (L29).

Response: Thanks for this comment, Fig.1 has been revised and posted in Line 100 in the revised manuscript. The 'box' of the Robeson Channel is shortened according to the figure in Kwok's paper (doi:10.1029/2005GL024768, 2005).

RC: L31 – "... that increased…"

Response: "that" has been added into the sentence in Line 32 in the revised manuscript.

RC: L34 – fluctuation of 0.43?... what does fluctuation mean? Standard deviation? Range? Pls use statistical terminology

Response: It is the Standard Deviation and now it is specified in Line 34 in the revised manuscript.

RC: L35 – instead of 'structure in south of RC depended on the existing of landfast ice'. how about 'structure south of RC depended on the presence of landfast ice'?

Response: We used "presence" to replace "existing" in Line 36 in the revised version. Thanks.

RC: L40 – instead of 'crossing the RC' .. how about 'transiting RC'?

Response: Thank you for your advice. "transiting" is better so it is used in Line 41 in the revised version.

RC: L44 – leading? : : : how about ‘caused’?

Response: “caused” is used instead of “leading by” in Line 45 in the revised version.

RC: L46 – ocean currents

Response: Yes. It has been modified in Line 48 in the revised manuscript.

RC: L47 – reduces

Response: The sentence is now modified to “Internal stresses, ..., reduce ice momentum.”, starting from Line 48 in the revised manuscript.

RC: L48 – what do you mean by ‘based on’? .. it is not clear what point you are trying to make here regarding spatial and temporal scales. Do you mean ‘is assessed at a variety’ of spatial and temporal scales?

Response: Yes. The sentence is now modified to “The dynamics of the ice motion can be assessed at a variety of spatial and temporal scales, ...” starting from Line 50 in the revised manuscript.

RC: L53 – it is unclear what ‘redistribution’ means here. Do you mean the floes collide, fracture and then produce a smaller floe size distribution?…or they drift and redistribute (causing re-orientation) themselves spatially? Pls clarify.

Response: Thanks for your suggestion. The sentence was modified to “the response to wind is usually manifested in floe-to-floe bumping, causing ridging, fracturing, floe breaking, re-orientation and differential motion”. This sentence starts from Line 55 in the revised manuscript.

RC: L59 - there is a period where I think you meant a comma

Response: There is a period after “ .. at 6.5 GHz.” We think it is correct.

RC: L74 - Begin the sentence with ‘In this study, : : :”

Response: The sentence now begins with “In this study, ...” in Line 81 in the revised version. Thanks.

RC: L75 – ‘The study includes a detailed…’

Response: “a” has been added into the sentence from Line 82 in the revised manuscript.

RC: L78 – How about saying ‘process mechanisms’ instead of ‘features’ .. since ice drift is not really a ‘’feature”.

Response: Yes. According to your suggestion, “features” is replaced by “process mechanisms” in Line 85 in the revised version.

RC: L82 – Its unclear where ’10 days’ comes from? Why not just say ‘development until maturity’ : : : and save the ’10 days’ for either the Results or Discussion section.

Response: Thank you for the suggestion. “10 days of” is deleted in Line 92 in the revised manuscript.

RC: L109 – this phrasing is odd : : : how about “This location is reasonably close in proximity and thus is the best available automated weather station to characterise the wind general wind field at a temporal resolution of one hour”.

Response: Thanks for this better phrasing. We have modified it to “This location is reasonably close to the Robeson Channel, and is thus the best ground source to characterize the general wind field at a temporal resolution of one hour”, starting from Line 124 in the revised version.

RC: L137 – ‘Sample maps’ ? : : : do you mean ‘Simple maps’?

Response: A new sentence is introduced: “The maps were generated at a spatial resolution of 1/12 × 1/12°, and both parameters were used to support the interpretation of the ice floe drift when it could not be explained by wind data only”. It starts from Line 157 in the revised version.

RC: L145 – “: : : into a polynya-like : : :”

Response: Thanks for the suggestion. “in” is changed to “into” in Line 165 in the revised manuscript.

RC: L182 – is it not possible to find any other study to support the observation that largescale motion of the pack ice .. other than an Arctic Council, 2001 report?

Response: In the revised version we use another reference in Line 250 in the revised manuscript:

Kwok, R., Spreen, G., and Pang, S.: Arctic sea ice circulation and drift speed: Decadal trends and ocean currents, J. Geophys. Res. Oceans, 118, 2408–2425, https://doi:10.1002/jgrc.20191, 2013.

RC: L188 – not why you are starting now to write out large numbers (ie. thirty-nine). Pls stay consistent here.

Response: Thanks for your suggestion. We follow the requirement of TC:

- **Numbers**
  - For items other than units of time or measure, use words for cardinal numbers less than 10; use numerals for 10 and above (e.g. three flasks, seven trees, 6 m, 9 d, 10 desks).

We use words less than 10, use numerals for 10 and above. All the numbers in the manuscript has been checked and modified now.

RC: L200 Figure 4 caption – 'slow motion upstream of the channel'

Response: "of" has been added into the sentence in Line 223 in the revised manuscript. Thanks.

RC: L204 – "Upstream of the RC…"

Response: "of" has been added into the sentence in Line 227 in the revised manuscript. Thanks.

RC: L210 – "The situation is difference for the floes that drifted within…" Figure 5 caption: : : do not say 'floated' .. say 'drifted' instead.

Response: Thanks. We have changed it in Line 246 in the revised manuscript.

RC: L251 – "Ocean current is remarkably weak…" .. or "Ocean currents are remarkably weak".. your choice.

Response: We change it to "... the ocean current is very weak …." in Line 300 in the revised manuscript.

RC: Table 2 caption – "…two successive daily Sentinel-1 SAR images" : : : also, there is no space in Floe#2 in table…that is there in Floe #3

Response: The space has been added in Table 2, in Line 349 in the revised manuscript.

RC: L479 – "In two occasions, …"

Response: It has been modified to "On two occasions, ..." in Line 519 in the revised manuscript.

RC: L512 – how about use the word concave : : : instead of dome shape

Response: Thanks for your suggestion. "concave" is better to describe the shape and it has been used instead of "dome" in Line 553 in the revised manuscript.

Sea Ice Drift and Arch Evolution in the Robeson Channel Using the Daily Coverage of Sentinel-1 SAR Data for the 2016–2017 Freezing Season

Mohammed E. Shokr[1], Zihan Wang[2], Tingting Liu[2]

[1]Meteorological Research Division, Environment and Climate Change Canada, Toronto, Ontario, Canada, M3H-5T4
[2]Chinese Antarctic Center of Surveying and Mapping, Wuhan University, Wuhan, 430079, China

Correspondence: Tingting Liu (ttliu23@whu.edu.cn)

Abstract. The Robeson Channel is a narrow sea water passage between Greenland and Ellesmere Island in the Arctic. It is a pathway of sea ice from the central Arctic and out to Baffin Bay. In this study, we used a set of daily synthetic aperture radar (SAR) images from the Sentinel-1A/1B satellites, acquired between September 2016 and April 2017, to study the kinematics of individual ice floes as they approach and then drift through the Robeson Channel. The tracking of 39 selected ice floes was visually performed in the image sequence and their speed was calculated and linked to the reanalysis 10-m wind from ERA5. The results show that the drift of ice floes is very slow in the compact ice regime upstream of the Robeson Channel, unless the ice floe is surrounded by water or thin ice. In this case, the wind has more influence on the drift. On the other hand, the ice floe drift is found to be about 4–5 times faster in the open drift regime within the Robeson Channel, and is clearly influenced by wind. A linear trend is found between the change in wind and the change in ice drift speed components, along the length of the channel. Case studies are presented to reveal the role of wind in ice floe drift. This paper also addresses the development of the ice arch at the entry of the Robeson Channel, which started development on 24 January and matured on 1 February 2017. Details of the development, obtained using the sequential SAR images, are presented. It is found that the arch's shape continued to adjust by rupturing ice pieces at the locations of cracks under the influence of the southward wind (and hence the contour kept displacing northward). The findings of this study highlight the advantage of using the high-resolution daily SAR coverage in monitoring aspects of sea ice cover in narrow water passages where the ice cover is highly dynamic. The information will be particularly interesting for the possible applications of SAR constellation systems.

1 Introduction

One of the exit gates for sea ice flux from the Arctic Basin to southern latitudes is through the Robeson Channel. The Robeson Channel is located between Greenland and Ellesmere Island (Canada), with its northern location around 82° N, 60.5° W (Fig. 1). It connects the Lincoln Sea (a southern section of the Arctic Ocean) to the Kennedy Channel, which opens into the Kane Basin. These three water bodies are known as the Nares Strait, which opens southward to Baffin Bay. The Robeson Channel is a short and narrow passage (about 80 km in length and 30 km wide) that is more than 400 m deep along its axis.

Oceanographic measurements in the Robeson Channel have not been routinely performed. Herlinveaux (1971) found the dominant surface current to be from north to south in April and May, with an average velocity that increased from about 0.36

Commented [1]: Instead of "Formation"

Commented [2]: Added

Commented [3]: Instead of "During"

Commented [4]: To Reviewer 2: The misspelled word "Metreological" is corrected.

Commented [5]: Instead of "formation process".

Commented [6]: To Reviewer 1: The wind direction are described as "southward", "northward" ..., instead of "northerly", "southerly" ... Wre are consistent with wind direction now.

Commented [7]: The longitude of RC's inlet is corrected.

Commented [8]: To Reviewer 2: "that" is added here.

km h^{-1} near the surface to nearly 0.9 km h^{-1} at a depth of 80 m. A strong southerly current of around 1.08 km h^{-1} was also measured in the western section of the channel during the early spring of 1971 and 1972, with a standard deviation of 0.43 (Godin, 1979). After using two ocean simulations to study the circulation and transport within the Nares Strait, Shroyer et al. (2015) found that the mean current structure south of the Robeson Channel depended on the presence of landfast ice.

Commented [9]: To Reviewer 2: Specify the meaning of "fluctuation".

Commented [10]: To Reviewer 1 & 2: Instead of "existing".

The sea ice cover in the Robeson Channel comprises a combination of seasonal (first year ice, FYI) and perennial ice (multi-year ice, MYI), both imported from the Arctic Basin through the Lincoln Sea. The only locally grown ice is found in narrow strips adjacent to the land at the two sides of the channel. Based on earlier results for ice thickness and motion retrieved from optical satellite sensors and reconnaissance flights in the 1970s, Tang et al. (2004) estimated the ice flux transiting the Robeson Channel to be around 40×10^3 km^2. Using a record of ice displacement retrieved from RADARSAT-1 images during 1996–2002, Kwok (2005) found the average annual ice area flux to be 33×10^3 km^2. Rasmussen et al. (2010) modelled the sea ice in the Nares Strait using a three-dimensional coupled ocean (HYCOM) and sea ice model (CICE). Their results showed a much lower ice flux in 2006 (20 km^3 $year^{-1}$) than in 2007 (120 km^3 $year^{-1}$), which caused blocking of the ice flow in the spring of 2006.

Commented [11]: To Reviewer 2: Instead of "crossing", better expression.

Commented [12]: To Reviewer 2: Instead of "leading by".

Sea ice drift is influenced by wind forcing, ocean currents and internal stresses within the pack ice. Internal stresses, which are caused by the interactions between ice floes and determined by the ice types and concentrations within the pack, reduce ice momentum. Other minor factors include the Coriolis force and sea surface tilt. The dynamics of the ice motion can be assessed at a variety of spatial and temporal scales (McNutt and Overland, 2003), namely, individual-floe (<1 km), multiple-floe (2–10 km for up to 2 days), aggregate-floe (10–75 km with a 1–3 d time scale), pack ice cover (75–300 km at 3–7 d) and sub-basin (300–700 km at 7–30 d) scales. The best coupling with wind occurs at the pack ice scale (also called the coherent scale). According to this categorization, only the individual- and multiple-floe scales can be observed in synthetic aperture radar (SAR) images of the Robeson Channel. In this case, the response to wind is usually manifested in floe-to-floe bumping, causing ridging, fracturing, floe breaking, re-orientation and differential motion (McNutt and Overland, 2003).

Commented [13]: To Reviewer 2: Instead of "current".

Commented [14]: To Reviewer 2: The sentence is modified for better expression.

Commented [15]: To Reviewer 2: Instead of "is based on".

Commented [16]: To Reviewer 2: Instead of "ridging, redistribution and differential floe motion", better expression.

Tracking individual ice floe motion from a sequence of satellite images is potentially feasible if the temporal resolution of the satellite coverage is sufficient (at least daily). An early attempt was reported in Sameleson et al. (2006) for ice in the Nares Strait using coarse-resolution satellite data (tens of kilometres) from a passive microwave radiometer at 6.5 GHz. The authors tracked the motion using only three to five locations of the same ice floe in a sequence of satellite images. Vincent et al. (2013) used Advanced Very High Resolution Radiometer (AVHRR) data (with frequent passes in the polar region) to track the motion

of the ice floes in the Nares Strait. However, due to the coarse resolution of the sensor, the results did not demonstrate the motion of individual ice floes.

Commented [17]: To Reviewer 1: We have checked and added this paper.

Due to their fine resolution (tens of metres), sequential SAR images are the best tool to monitor sea ice kinematics, particularly if available at a short time scale. However, SAR data have a limited spatial coverage. The earliest studies to estimate sea ice displacement using SAR data were presented in Hall and Rothrock (1981) and Leberl et al. (1983), using sequential Seasat SAR images. Later, making use of the more frequent coverage of RADARSAT-1 in the western Arctic, the Radar Geophysical Processing System (RGPS) was developed and produced gridded ice motion and deformation data, tracked every 3–6 days from 1998 to 2008 (Kwok and Cunningham, 2002). A more recent ice tracking operational system (also gridded) was described in Demchev et al. (2017), using a series of Sentinel-1 SAR images.

While the Robeson Channel is covered most of the year by an influx of ice from the Lincoln Sea, the flow of the ice is sometimes blocked in the winter at the entrance of the channel by the formation of an arch-shaped ice configuration that spans a transect between two land constriction points at Greenland and Ellesmere islands. The arch usually collapses in early summer, allowing continuation of the ice flux. Kwok et al. (2010) pointed out that no arch was formed in 2007, leading to a major loss of Arctic ice, which was equivalent to about 10% of the average annual amount of ice discharged through the much wider Fram Strait (400 km versus 30 km width). This signifies the fact that the entire Nares Strait could represent a major route to the Arctic if the ice arch ceases to form in the future due to the thinning of Arctic ice. Moore and McNeil (2018) addressed the collapse of this arch in relation to the recent trend of sea ice thinning. In this study, the arch formation started on 24 January 2017 and continued until May 2017. The paper includes a detailed description of the mechanism of the arch's development.

Commented [18]: To Reviewer 2: Instead of "In the present data set".

Commented [19]: To Reviewer 2: Added here.

The objective of the study was to utilize the daily Sentinel-1A/1B SAR coverage of the Robeson Channel area during a full freezing season (September 2016 to end of April 2017) to examine two sea ice process mechanisms in the Robeson Channel. The first was the drift of individual ice floes, in terms of speed and direction. For this purpose, 39 ice floes were selected and each floe was tracked manually in the series of available Sentinel-1 images. The motion information was linked to the 10-m wind reanalysis data to explore the influence of wind on the ice drift. When wind did not explain the ice motion, an explanation in terms of other factors, namely, ocean current, surrounding ice concentration, tidal forces and to a much lesser extent the sea surface height (SSH) was considered. Knowledge about how wind and ice drift are related enables the improvement of sea ice/atmosphere dynamic models (Leppäranta, 2011). The second process was monitoring the development of the ice arch at the inlet of the Robeson Channel during its development until maturity. The advantage of using the daily coverage of the fine-

Commented [20]: To Reviewer 2: Instead of "features".

Commented [21]: These factors are considered only when wind does not explain the observed ice drift.

Commented [22]: To Reviewer 2: "10 days of" is deleted.

resolution SAR data in retrieving this information in such a narrow channel is expected to instigate further operational applications of SAR constellation systems (e.g. the recent Canadian RADARSAT Constellation Mission (RCM)) with their finer temporal resolutions. It should be noted that operational ice drift products are generated based on cross-correlation between sequential images, which is a statistical approach, while the current approach is based on the manual identification of individual ice floes. Admittedly, this task is laborious, but the motion product has a superior accuracy and can be linked to a detailed dataset of reanalysis wind.

Commented [23]: Address the advantage of manually identified ice motion data.

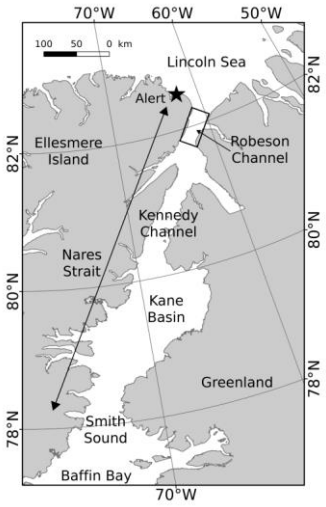

Figure 1. Map of the Robeson Channel and its surrounding areas. The Robeson Channel is located between Greenland and Ellesmere Island (Canada), with its northern location around 82° N, 60.5° W. It connects the Lincoln Sea to the Kennedy Channel, which opens into the Kane Basin.

Commented [24]: To Reviewer 2: The box showing the boundary of RC has been modified. So now it has roughly 80 km length along its axis.

2 Datasets

2.1 Satellite data

Sentinel-1A and 1B are two satellites developed within the satellite constellation of the European Space Agency's (ESA) Copernicus program. They were launched on 3 April 2014 and 25 April 2016, respectively. Both carry a carbon-copy C-band SAR sensor (with a central frequency of 5.405 GHz) with a selection of single or dual polarization. Image acquisition is

performed in one of four operation modes: Stripmap (SM), Interferometric Wide swath (IW), Extra-Wide swath (EW) and Wave (WV). The IW (swath width 250 km at a spatial resolution of 5 × 20 m) and EW (swath width 400 km at a median resolution of 20 × 40 m) modes were used in this study, which are both Level-1 Ground Range Detected (GRD) products. All the images were acquired in HH polarization. An almost daily coverage of the Robeson Channel area from both satellites was obtained from late September 2016 to the end of April 2017 (a total of 361 images). The images were calibrated to give backscatter coefficients in decibels, and were then georeferenced. In order to reduce the image size and the speckle, the images were resampled to 50 × 50 m. While the incidence angle of the EW mode varies between 29.1° and 46.0° across the swath, no correction for the variation of the angle was performed since the backscatter was not used quantitatively.

2.2 Wind data

Reanalysis of 10-m level wind is available from a few sources. Four sources were examined in this study: (1) the U.S. National Centers for Environmental Prediction/National Center for Atmospheric Research (NCEP/NCAR) reanalysis project (Kalnay et al., 1996); (2) the NCEP/Department of Energy (NCEP/DOE) reanalysis model (Kanamitsu et al., 2002); (3) the European Centre for Medium-Range Weather Forecasts (ECMWF) reanalysis (ERA-Interim) (Dee et al., 2011); and (4) its successor ERA5 (C3S, 2017). The specifics of each source are presented in Table 1. The difference between the estimated speed from each source and the speed from the Arctic Alert station is plotted in Fig. 2 for the period from 1 October 2016 to 30 April 2017. The Arctic Alert weather station (Canada) is located at (82.52° N, 62.28° W). This location is reasonably close to the Robeson Channel, and is thus the best ground source to characterize the general wind field at a temporal resolution of one hour (Fig. 1).

Commented [25]: To Reviewer 2: The sentence is modified.

Figure 2 reveals the overestimation of the reanalysis wind when the station's wind measurement is <10 km h^{-1}. As the wind measured from the station increases, a systematic underestimation of the reanalysis wind can be observed. This is particularly true of the two ERA products. When the speed from the Alert station exceeds 30 km h^{-1}, the reanalysis wind from all sources can be severely underestimated by as much as 20–40 km h^{-1}. Previous studies have shown that the low-resolution global reanalyses of the wind speed and direction have large errors in the narrow channels of the Nares Strait (Dumont et al., 2009). The present data show that the average absolute deviation of the NCEP/NCAR, NCEP/DOE, ERA-Interim and ERA5 wind reanalysis from the measured wind at the Alert station is 9.12, 9.74, 9.04 and 8.92 km h^{-1} over the period from 1 October 2016 to 30 April 30 2017. Hence, we chose the ERA5 data because of its minimum deviation from the Alert station data and the finer grid spacing. The data were used to explore links with the ice floe drift and to study the ice arch development. The grid points from the ERA5 reanalysis relevant to the study area are shown in Fig. 3. Data from the appropriate grid points are introduced later in the relevant sections.

Table 1. Information about the available wind data for the study area from the Arctic Alert weather station and the four sources of reanalysis data.

Data	Alert stn.	NCEP/NCAR	NCEP/DOE	ERA-Interim	ERA5
Grid spacing	-	2.5 × 2.5°	1.88 × 1.90°	0.75 × 0.75°	0.25 × 0.25°
Temporal res. (h)	1	6	6	6	1
Level (m)	10	10	10	10	10
Nearest grid pt. to Alert stn. (km)	-	37.6	37.6	1.9	1.9

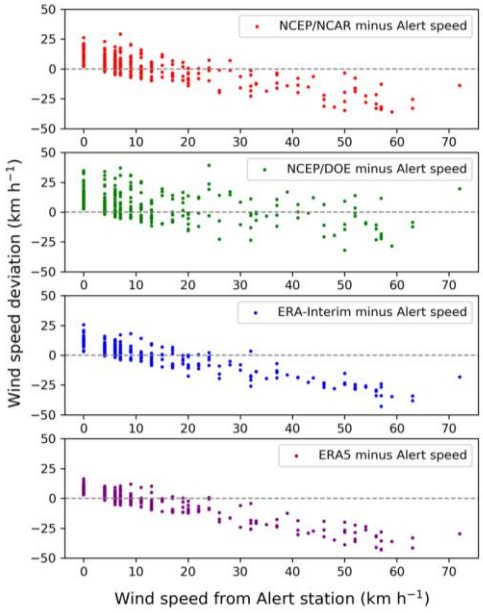

Figure 2. Deviation of the reanalysis wind speed from the speed measured at the Arctic Alert weather station (reanalysis wind minus station wind) for the period 1 October 2016 to 30 April 2017. The reanalysis data are from NCEP/NCAR, NCEP/DOE, ERA-Interim and ERA5.

Note the increasing underestimation of the reanalysis data as the measured wind increases. Units of the x-axis in the bottom segment apply to all segments.

Commented [26]: To Reviewer 1: The unit is added into the caption.

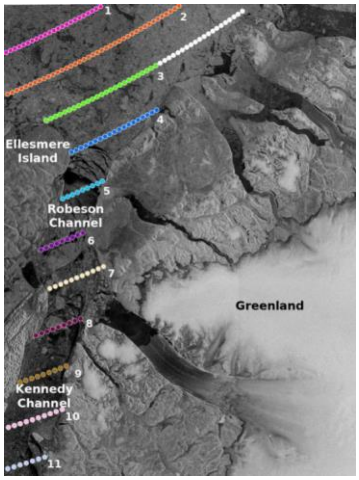

Figure 3. ERA5 grid points of the wind reanalysis data used in the present study. The background is the Sentinel-1B image acquired on 30 January 2017.

2.3 Ocean current and sea surface height (SSH)

Daily and monthly mean maps of ocean current (vertical coverage at 50 levels from −5500 m depth to surface) and SSH are components of the GLORYS12V1 reanalysis product covering the satellite altimetry era (1993–2018). This is based on the real-time ocean reanalysis product of the Copernicus Marine Environment Monitoring Service (CMEMS) (Fernandez and Lellouche, 2018; Lellouche et al., 2018). The maps were generated at a spatial resolution of 1/12 × 1/12°, and both parameters were used to support the interpretation of the ice floe drift when it could not be explained by wind data only.

Commented [27]: To Reviewer 2: The sentence is changed for better expression.

3 Method

The daily fine-resolution images of Sentinel-1A/1B (50 m) were used to generate tracking of the selected sea ice floes and to detect the temporal evolution of the ice arch from its commencement on 24 January until it matured on 1 February 2017. In total, 39 ice floes were tracked between 26 September 2016 and 11 April 2017. A total of 32 ice floes moved mainly southward,

Commented [28]: To Reviewer 1 & 2: Instead of "thirty-nine". According to TC's guide, we use words for number less than 10 and use numerals for 10 and above.

crossing the inlet of the Robeson Channel, and seven moved mainly northward within the Robeson Channel. Among the seven ice floes, five moved in the drifted ice regime before and shortly after the formation of the ice arch, and two moved into a polynya-like regime after the formation of the arch. Each ice floe was visually identified in a sequence of daily SAR images (between 11 to 54 sequential scenes), and then the ice floe displacement, drift speed and direction were calculated. The displacement was determined from the subjectively estimated locations of the same ice floe in two successive daily images, using a code to convert latitude/longitude pairs to distance according to the World Geodetic System (WGS84) coordinate system.

Three sources of error were implied in the estimation of the displacement. The first was the geolocation error of the SAR imagery. The Sentinel-1 product specification (Bourbigot et al., 2016) mentions that the absolute pixel location accuracy is less than 7 m for the IW mode, but no figure is given for the for EW mode, which was used in this study. The second source of error was the assumption of a linear path (as opposed to a curvilinear or meandering path) for the ice floe between two successive days. This assumption had to be employed because the temporal resolution of Sentinel-1A/1B is not finer than one day. The pattern of ice floe motion depends primarily on the changing wind direction and the mechanical properties of the surrounding ice floes. The third source of error was the subjective estimate of the centroid of the same ice floe in successive images. This was also estimated to be within a few pixels. Assuming that these errors were independent and normally distributed, the error in the estimated ice drift speed would be roughly 0.2 km d^{-1}.

The ice floe speed was calculated using the travelled distance, as mentioned above, and the period between the two successive image acquisitions, which varied between 16 and 33 hours. To link the ice floe speed to the wind at any ice floe location, the reanalysis wind values from ERA5 for the four grid points closest to the floe were averaged. This was done to avoid the inclusion of wind data from grid points far from the relevant ice floe location, which can be often be very different. The 3-hour wind vectors that acted on the given ice floe during its transition in the period of the two satellite passes were produced in the form of polar maps, to qualitatively explore their influence on the ice floe drift. In addition, the 3-hour wind speeds from the four grid points around each ice floe at each location were averaged to quantitatively link to the drift speed. Statistics were then generated to quantify the wind influence.

The evolution of the ice arch from its onset of formation on 24 January until its maturity on 1 February 2017 was manually delineated in each image. The daily displacement of the two end points of the ice arch was calculated using the latitude/longitude coordinates. To investigate the role of the wind on the progress of the arch shape, as well as the location and

Commented [29]: To Reviewer 2: Instead of "in".

Commented [30]: The numbers are corrected.

Commented [31]: Supplement

Commented [32]: This sentence has been improved.

displacement of its terminal points, daily wind data from the ERA5 reanalysis were averaged from the 3-hour intervals at the coloured grid points from lines 3, 4 and 5 (corresponding to latitudes 82.5° N, 82.25° N and 82° N, respectively) in Fig. 3.

Commented [33]: Corresponding latitudes are added.

4 Results

The ice floe motion and arch formation are addressed in two subsections. The ice floe motion is considered in two separate regimes: north of the Robeson Channel near its entrance and within the Robeson Channel. In the first regime, the ice floes approach the Robeson Channel in a convergent path forming pack ice cover, which is a term used when ice concentration exceeds 70%. On the other hand, the ice regime within the Robeson Channel falls into the category of drifted ice, a term used to denote an ice concentration of less than 60%. The two regimes feature different ice floe drift patterns, and the influence of the wind also differs, as explained later. Case studies of the ice floe motion are presented for each regime to reveal the quantitative and qualitative information about the wind influence. In the second subsection, the role of the wind on the evolution of the ice arch at the inlet of the Robeson Channel is addressed.

Commented [34]: To Reviewer 1: The whole paragraph has been rewritten for easier understanding.

4.1 Ice floe motion

4.1.1 Tracking ice floe drift

Commented [35]: To Reviewer 2: The reference of Arctic Council (2001) is deleted and we added another reference in Section 4.1.3.

The ice flux transiting the Robeson Channel encompasses ice floes of different ages and sizes. The typical dimensions of the ice floes examined in this study ranged from 2 to 16 km. Some ice floes were aggregates of smaller floes, which disintegrated during their journey. The 39 ice floes selected for motion tracking in the Sentinel-1 images were numbered, and the numbers are used in the following analysis, although the order does not carry any significance. The tracks of 12 ice floes are shown in Fig. 4, with the floe numbers and the dates at each position attached. These ice floes were mostly heading southward, but with a few interruptions to this dominant direction. The high ice concentration in the convergent path upstream of the Robeson Channel caused reduction of the ice motion and induced meandering paths. However, in areas with less ice concentration, the ice floe motion accelerated and became more influenced by wind, as will be demonstrated in case study 1. Once the ice floes crossed the bottle neck at the entrance to the Robeson Channel, they became partially relieved from the stresses induced by the surrounding ice and more responsive to other factors such as wind and current. Thus, the speed increased greatly by a factor of 1.5–5, and the drift direction followed mostly the north–south extension of the Robeson Channel, which coincided with the dominant wind direction. This direction also coincided with the dominant ocean current direction. Figure 4 also shows that the ice floes did not enter any of the fjords at the sides of the channel. In fact, many fjords become filled by locally grown landfast ice early in the freezing season.

Commented [36]: This sentence has been improved.

Commented [37]: To Reviewer 1: These sentences are rewritten for easier understanding of readers.

Commented [38]: To Reviewer 1: We use specific number instead of “remarkably”. All the “remarkably” is deleted from the manuscript.

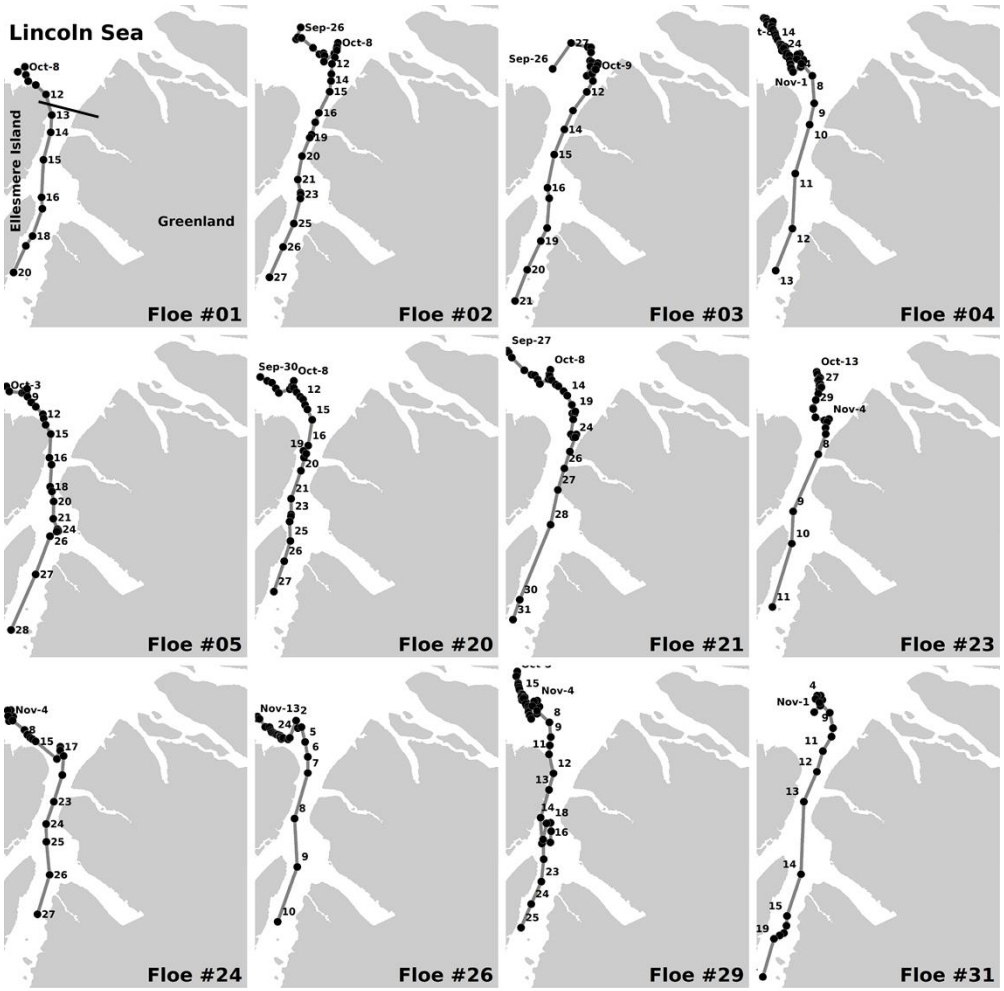
Lincoln Sea
Ellesmere Island
Greenland
Floe #01
Floe #02
Floe #03
Floe #04
Floe #05
Floe #20
Floe #21
Floe #23
Floe #24
Floe #26
Floe #29
Floe #31

Figure 4. Trajectories of 12 selected ice floes, obtained from the daily Sentinel-1 images, as they approach and pass through the Robeson Channel. Note the slow motion upstream of the channel and the faster motion through the channel. The entrance to the channel is marked by the solid line in the top left panel.

Commented [39]: To Reviewer 2: Added here.

4.1.2 Ice floe drift speed

Figure 5 shows the average drift speed of each ice floe (regardless of drift direction) during its entire observation time in the SAR time series, either upstream or within the Robeson Channel. Upstream of the Robeson Channel, the drift speed varied within a narrow range (4–10 km d^{-1}), with a typical value around 5 km d^{-1}. Such nearly constant drift speeds, observed under different wind speeds, suggest that the wind has a minor influence or even no influence on the ice floe drift in this area. The exceptionally high average speed of ice floe #6 (~19 km d^{-1}) resulted when the floe drifted in a surrounding area of nearly zero ice concentration, which prevailed for three days.

Commented [40]: To Reviewer 2: Added here.

Commented [41]: Instead of "from".

The situation was different for the ice floes that drifted within the Robeson Channel. Here, the ice floe speed was much higher, typically between 14 and 45 km d^{-1}. One ice floe reached an extreme speed of around 99 km d^{-1} on one day, as shown in case study 3 below. The higher drifting speed inside the Robeson Channel can be partly explained by the low ice concentration and/or the prevalence of thin ice, particularly after the ice arch matured on 2 February 2017. Both factors gave rise to a more significant influence of wind and ocean currents on the ice drift. The large variability of the ice floe speed within the Robeson Channel, which contrasts with the nearly constant speed upstream of the Robeson Channel, can be attributed to the influence of the variable wind speed and direction. For example, the very high average speed of ice floe #4 (45 km d^{-1}, as shown in Fig. 5), which is a manifestation of the large leap in location during the period 10–13 November (Fig. 4), was instigated by a dominant southward wind between 20 and 40 km h^{-1} during that period. On the other hand, the relatively slow average drift speed of ice floe #5 (15 km d^{-1}, as shown in Fig. 5) resulted from a reversed wind direction that blew from south to north at 10–20 km h^{-1} between 18 and 26 October. This adverse wind neutralized the action of the southward current.

Commented [42]: This sentence has been improved.

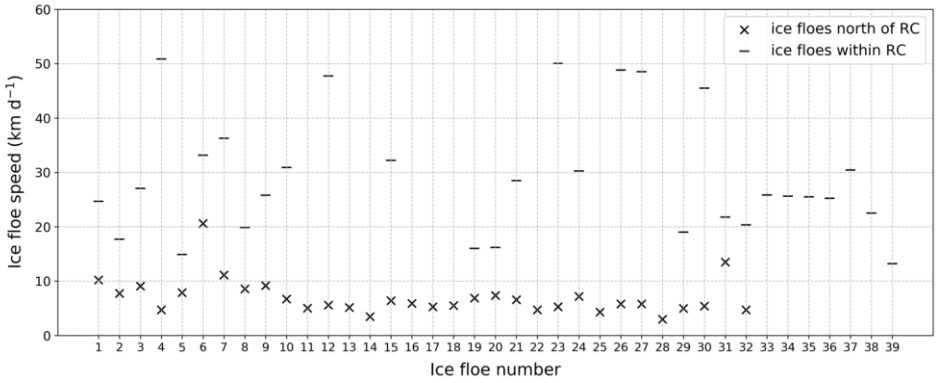

Figure 5. Average speed of individual ice floes during the periods upstream and within the Robeson Channel. The last seven floes (#33–39) drifted within the Robeson Channel with highly variable speeds.

Commented [43]: To Reviewer 2: Instead of "floated".

Commented [44]: To Reviewer 1 & 2: The whole paragraph is rewritten thoroughly and describes our exploration of tidal effects on ice drift. Due to lack of regular generation of tidal data in this area，no confirmed conclusion could be obtained from this dataset on how tide impacts ice drift in the Robeson Channel.Detailed information can be found in the Response Letter.

4.1.3 Driving forces of ice floe motion

While several studies have confirmed the coherency between wind forcing and the large-scale motion of pack ice, the results presented in this section are focused on examining the influence of wind on the drift of individual ice floes. For the large-scale motion of the pack ice in the Nares Strait, Kwok et al. (2013) confirmed that this was triggered by both ocean current and wind, which pushed the ice from the Lincoln Sea southward to the Robeson Channel. As mentioned in Section 1, ice dynamics at the floe- and multiple-floe scales is triggered by a combination of wind, ocean current, internal stress within the pack ice, the Coriolis force, SSH and tidal forces. In the following presentation, when the wind is not found to be linked to the observed ice motion, other factors are considered. A few points about some of these key factors are reviewed here.

Ice concentration is used as a proxy indicator of internal forces within the pack ice. In this study, this parameter was visually estimated from the SAR images. In close pack ice (ice concentration >70%), the influence of the internal forces overrides other factors such as wind and current, as shown in case study 1. On the other hand, when ice moves in a drifted ice regime with a low ice concentration, which is the case within the Robeson Channel, the effect of the wind and ocean currents becomes more pronounced. As mentioned above, the maps of ocean currents and SSH are available from the same source in daily and monthly average gridded products. An example of the monthly averaged data for December 2016 is shown in Fig. 6. This example is typical of the winter months. The surface current in the central path of the Nares Strait, including the Robeson Channel, is about five times faster than the typical current north of the Robeson Channel, and the dominant southward wind reaches speeds between 0.72 and 1.38 km h^{-1}. This would be powerful enough to influence the ice floe drift. We performed multivariate

regression analysis using the current and wind data from within the Robeson Channel to evaluate the relative weight of each factor. The SSH map for December 2017 (Fig. 6) reveals a decreasing gradient westward. This might suggest a limited impact on the ice floe motion, particularly north of the Robeson Channel (Wekerle et al., 2013).

Tide data in this region are not generated regularly. A few datasets are available, which were acquired during expeditions to measure other oceanic parameters. For example, Münchow et al. (2007) and Münchow and Melling (2008) measured ocean currents in the Nares Strait using mooring buoys, most of which were located at the southern end of the Kennedy Channel. They found that the tide impacted the dominant component of current in the Nares Strait. However, Münchow et al. (2007) indicated that the amplitude and phase of the tidal constituents varied substantially both along and across the strait. Meanwhile, Johnson et al. (2011) indicated that Petermann Fjord, at 81° N, is well above the critical latitude for the M2 tide (74.5° N). Since the Robeson Channel is above the latitude of Petermann Fjord, the tidal effect is assumed to have a much smaller influence on ice drift in the Robeson Channel than the other regimes in the Nares Strait. Gimbert et al. (2012) used the Fourier spectra of the buoy velocity from the International Arctic Buoy Program (IABP) to investigate the impact of the tidal effect in the Arctic Basin. We checked all the available buoy datasets and found that nine buoys operated in the Nares Strait during September to April, from 1979 to 2016. We calculated the Fourier spectra of the velocity records from each buoy and found different spectra from the different buoys, some with and others without peaks. The peaks may be linked to the regular pattern of the tide. Therefore, no confirmed conclusion could be obtained from this dataset on how tide impacts ice drift in the Robeson Channel.

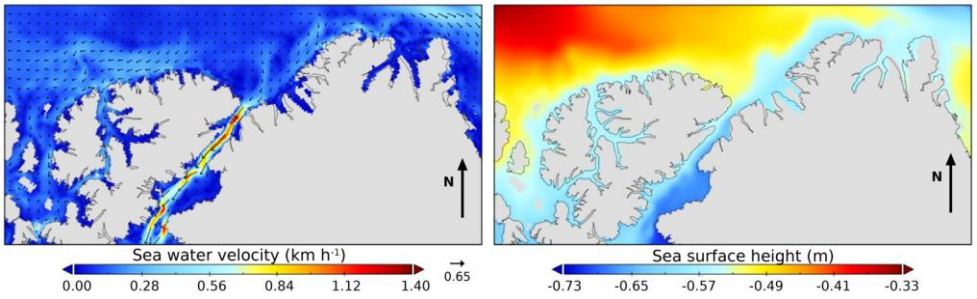

Figure 6. Maps of ocean current near the surface (left) and sea surface height (right), averaged over December 2016 from GLORYS12V1, which is generated by the Copernicus Marine Environment Monitoring Service.

1) Ice drift upstream of the Robeson Channel

Synoptic information about the ice regime north of the Robeson Channel is presented using the six selected scenes shown in the sequence of Sentinel-1 images in Fig. 7. A bulge-shaped area of consolidated ice appears to be attached to the coast of Greenland. It is delineated by the dotted lines in all the images, except in the image for 26 October, although it is still just visible in this image. This may possibly be a large extent of landfast ice, although it was exposed to cracking, as can be seen in the image for 7 November. An arch-like crack is visible in the image for 13 November, with its boundary coinciding with the bottom boundary of the landfast ice area. This was probably instigated by the strong southward wind (20–60 km h^{-1}) which prevailed on 8 November. However, this arch did not survive because its west-side terminal (left side in the image) was not anchored on land at this point. Further details of this phenomenon are presented in the next section.

Figure 7 shows that the ice entering the Robeson Channel follows a path coming around the north of Ellesmere Island, as shown by the arrow in the image for 1 December. No ice appears to be coming along the coast of Greenland. This large-scale motion is likely driven by the strong southward wind, which is channelled down the atmospheric pressure gradient from the Lincoln Sea to Baffin Bay (Gudmandsen, 2000), and the ocean current. However, since the ocean current is very weak in this area (Fig. 6), it is possible that the ice motion around the tip of Ellesmere Island is driven by the west–east gradient of the SSH (Fig. 6). Wekerle et al. (2013) mentioned that the SSH difference between the Arctic Ocean and Baffin Bay not only leads to a net outflow from the Arctic Ocean, but its variability also drives the variation of the Canadian Arctic Archipelago (CAA). As the ice cover approaches the entrance of the Robeson Channel, the ice floes demonstrate erratic motion (Fig. 4). This nullifies the possible influence of ocean current or SSH. The ice floe motion immediately upstream of the Robeson Channel appears to be mainly determined by the interactions between neighbouring ice floes in the closed pack ice. This observation is illustrated in the following case study.

Commented [45]: Sentences are rewritten for easier understanding.

Commented [46]: To Reviewer 1: The sentence structure is modified.

Commented [47]: Instead of "The pack ice motion is driven by".

Commented [48]: To Reviewer 1: These sentences are rewritten to show a possible influence of current SSH to ice drift. Detailed information can be found in the Response Letter.

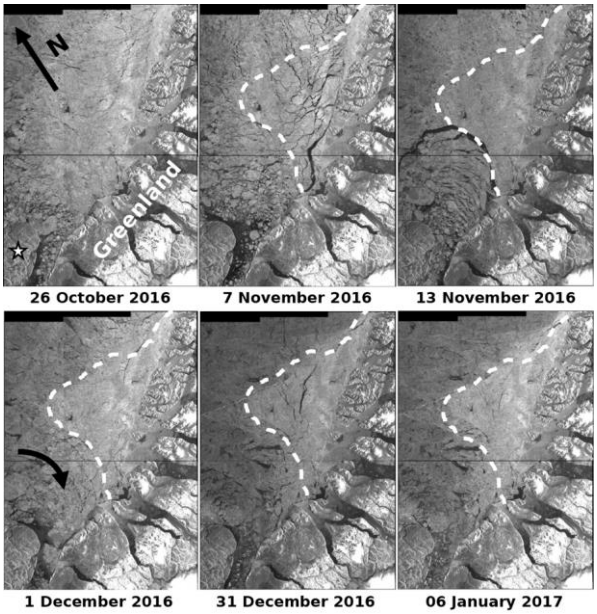

Figure 7. Sequence of Sentinel-1A/1B images for an area north of the Robeson Channel. The dotted curve marks an area of consolidated ice (still visible in the 26 October image). Ice cracked in this area on 7 November and an ice arch was formed on 13 November. The star in the middle panel of the top row marks Ellesmere Island. Ice floes that made their way to the Robeson Channel originate from the west (not north), following the path shown by the arrow in the 1 December image.

Commented [49]: To Reviewer 1: The misspelled word "bath" is corrected.

Case study 1: two floes drifting upstream of the Robeson Channel

Figure 8 shows sequential Sentinel-1 images (26 September to 7 October 2016) of a segment just upstream of the Robeson Channel, where two ice floes appear. Ice floe #2 is marked by the grey dot, a natural low backscatter area, and floe #3 is marked by the star. The corresponding maps of the 3-hour ERA5 reanalysis wind vectors are presented in Fig. 9. The daily speeds of each ice floe are listed in Table 2, along with the wind and qualitative concentration data. This information helps in defining the impact of the wind on the ice floe drift, as explained below.

Commented [50]: To Reviewer 1: Redundant information is deleted. And the sentence is rewritten for better expression.

Commented [51]: To Reviewer 1: We eliminated many of those parenthetical statements to make the reading flows better.

The image for 26 September shows the two ice floes surrounded by open water and thin ice. The wind between the two satellite overpasses on 26 and 27 September (averaging 33 km h^{-1}) was partly heading northeast or southeast. This relatively high wind,

combined with the less resistive ice in the surrounding, caused floe #3 to drift northeast at a top speed of 24 km d^{-1} (Table 2). Between 27 and 28 September, relatively light wind (<20 km h^{-1}) blew in the opposite direction, but floe #3 drifted southeast at 18.05 km d^{-1} because this path was the path of less resistance. Floe #2 did not move far with a drift speed of 2.84 km d^{-1} as it was surrounded by ice. Between 28 and 29 September, the light wind did not change and the two ice floes remained at the same locations. When the wind direction switched to the southeast between 29 and 30 September, with the speed reaching 30 km h^{-1}, the two floes drifted in the same direction, with floe #2 reaching a speed of 15.72 km d^{-1}, as shown in Table 2. Here, once again, the path was nearly ice-free. Between 30 September and 1 October, when a southwestward wind blew at nearly 30 km h^{-1}, the ice drift accelerated to nearly 9 km d^{-1}. After 1 October, the wind abated but the drift continued in a southeast direction at a moderate speed of 2–6 km d^{-1}. When the northward wind exceeded 40 km h^{-1} between 4–7 October, before it was reduced to less than 30 km h^{-1}, the ice floe drift did not follow the wind action in the first two days because the two floes were surrounded by high ice concentrations. Nevertheless, southwestward drift was observed between 4–5 October, particularly for floe #2 (Fig. 8), following the strong northwestward wind during the same period (Fig. 9). This case study demonstrates the effective role of wind on ice floe drift when the floe is surrounded by thin ice or water.

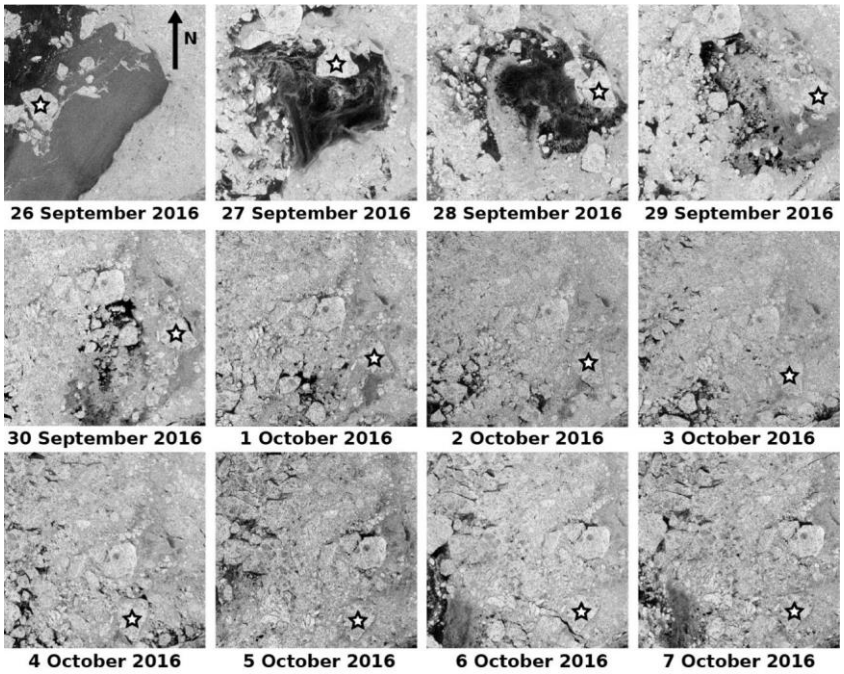

Figure 8. Sequential Sentinel-1A/1B images (dates are shown) showing the advancement of two ice floes. Floe #2 is marked by a grey dot (a natural low backscatter area), and floe #3 is marked by a star. The ice concentration surrounding each floe is visible and can be qualitatively estimated.

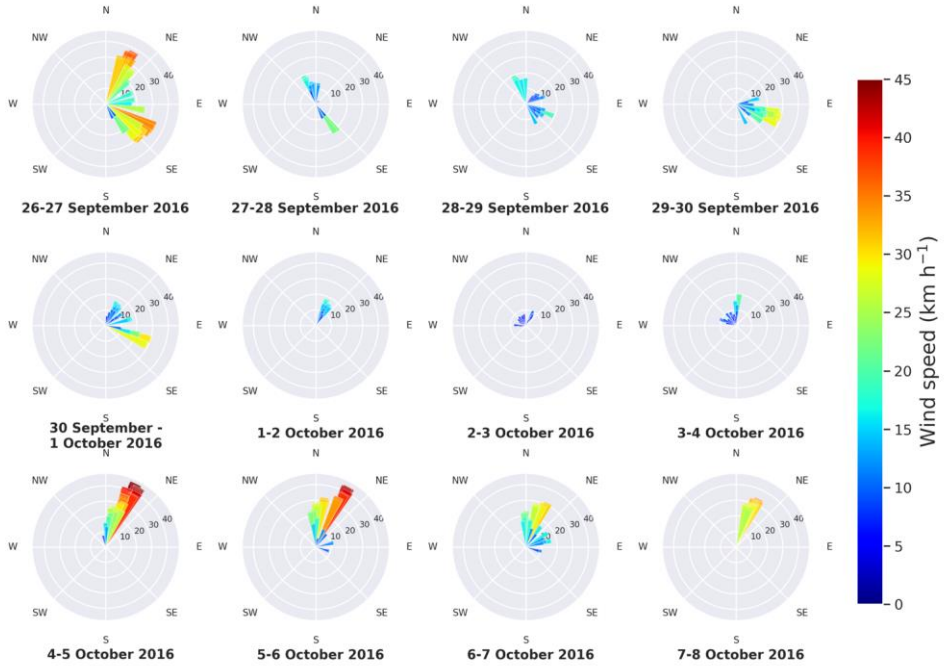

Figure 9. Maps of the 10-m level wind vector (km h^{-1}) from the ERA5 reanalysis. Each panel has vectors from the four grid points surrounding the locations of ice floes #2 and #3 every 3 hours during the time between the daily overpasses of Sentinel-1. For example, the 26–27 September panel shows the 3-hour vectors that were available between the period that spans the satellite acquisition times of 26 and 27 September.

Commented [52]: To Reviewer 1: The caption is modified to make it comprehensible.

Table 2. Drift speed of ice floes #2 and #3 (shown in Fig. 8) during the period between the acquisitions of the two successive daily Sentinel-1 images. The period is shown in the first column.

Date	Avg. speed (km d^{-1})		Wind speed (km h^{-1})	Qualitative ice concent.
	Floe #2	Floe #3		
26–27 September	9.68	24.17	33	low
27–28 September	2.84	18.05	15	low
28–29 September	3.97	3.32	10	low

Commented [53]: To Reviewer 2: Instead of "two successive Sentinel-1 coverage".

Commented [54]: To Reviewer 1: The unit has been corrected.

29–30 September	15.72	5.26	30	low
30 Sept.–1 Oct.	9.73	8.85	30	moderate
1–2 October	6.59	3.72	9	moderate
2–3 October	2.62	4.59	4	high
3–4 October	6.26	4.58	5	high
4–5 October	10.46	4.39	30	high

2) Ice drift within the Robeson Channel

Prior to the formation of the ice arch on 24 January 2017, the channel was filled with ice floes transported from the north. Shortly after the development of the ice arch, the channel became covered with thin ice and open water, which is typical of polynya cover. In both situations, the direction of the ice floe motion was mainly north–south, following the dominant wind and current directions, although the wind was occasionally reversed (Fig. 4). The low ice concentration (<40%) in this drifted ice regime enhanced the roles of all the factors impacting the ice motion, particularly the wind and ocean current. In the absence of other factors, the role of the wind is examined through the scatter plot of the wind and ice motion components in the north–south direction, as shown in Fig. 10. The data points marked by the open circles in Fig. 10 represent floes number 1–37, which entered the Robeson Channel from the north prior to the arch formation, and the points marked by the closed circles are from the motion of floes #38 and #39. These two floes originated in the Robeson Channel after the arch formation, so they moved freely in the thin ice/water field. Positive values indicate motion northward, and vice versa. It can be seen that a southward-blowing wind is always associated with southward ice drift. When the wind blows northward, the ice floes may remain drifting southward. In this case, the motion must be influenced by the southward ocean current. However, as the northward wind accelerates, the ice may eventually drift northward. This is shown in the reversed path of floe #29 between 10 to 18 November in Fig. 4.

The trend of the data points in Fig. 10 is defined by the linear regression equation $fs = 0.063\ ws - 0.98$, where *fs* and *ws* are the ice floe and wind speed, respectively. The slope of the regression line from the data of floes #1–37 (Fig. 10) shows that when the ice floe motion coincides with the wind direction, the flow speed becomes roughly 1/15 of the wind speed. This equation suggests that, in the absence of wind, the ocean current would induce floe drift (southward) at approximately 0.98 km h^{-1} (22 km d^{-1}). The coefficient of determination (R^2) of this regression is 0.565. The same coefficient increases to 0.679 from the data for floes #38 and #39 only. A higher R^2 means less variability in the data, and therefore a better regression model.

This means more influence of wind on ice motion when the ice is drifting in the polynya-like regime of thin ice and open water.

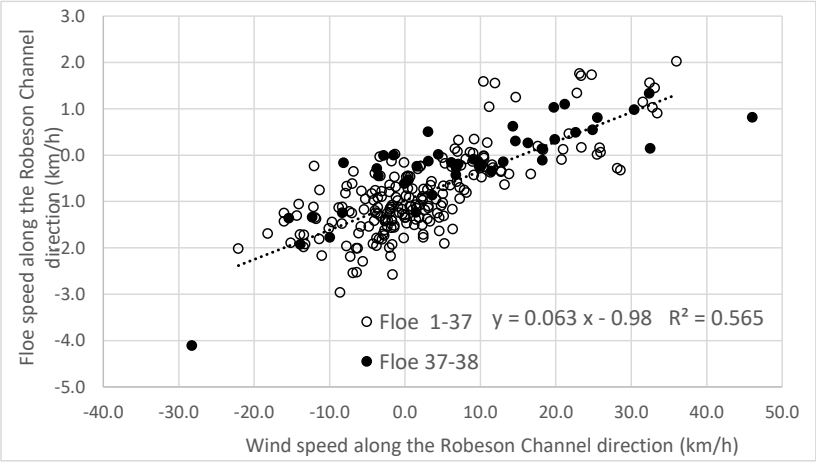

Figure 10. Scatter plot of wind versus ice floe speed components along the Robeson Channel direction. Positive and negative values pertain to wind or ice motion heading north or south, respectively. Data from 39 floes drifting within the Robeson Channel are shown. The open circles pertain to 37 ice floes that originated north of the Robeson Channel and then formed part of the drifted ice regime in the Robeson Channel (where many ice floes existed). The closed circles represent data from two floes that originated inside the Robeson Channel and then drifted in the polynya formed after the ice arch was formed. The dashed line is the linear regression for the data of the 37 floes.

Commented [55]: To Reviewer 2: Two paragraphs and the previous Figure 11 are deleted to shorten the manuscript.

Commented [56]: The following paragraph and Table 3 are added here using multiple linear regression to distinguish between the influence on ice drift from wind speed and current speed.

Isolating the wind and ocean current contributions to ice motion can be better achieved using a modelling approach, as presented in Thorndike and Colony (1982) and Kimura and Wakatsuchi (2000). However, in order to achieve this task using the present data of daily gridded wind and ocean current, we performed multivariate regression analysis, with the wind and current data as the independent variables and ice floe speed as the dependent variable. Only the components along the Robeson Channel extent were considered. The results are shown in Table 3. The standardized coefficient is a measure of how much an independent variable explains the dependent variable. In this case, the wind and current speed can explain 0.729 and 0.165 of the ice floe motion, respectively. Statistical significance is the probability of rejecting the null hypothesis, which is no significant difference between the contribution of wind and current, in this case. The Pearson correlation coefficient is a statistic that measures the linear correlation between two variables. Here, the wind shows a better linear correlation with the ice floe motion. The partial correlation coefficient is a measure of the correlation between the dependent variable and one independent

variable, in the absence of other independent variables. Once again, the results show the more significant contribution of the wind. The variance inflation factor (VIF) should be <10, otherwise there is severe multicollinearity in the model. The conclusion from these results is that wind speed has a greater influence on ice floe motion than ocean current in the open drift (40–60% ice concentration) or very open drift (<40% ice concentration) regimes in the Robeson Channel.

Table 3. Results from the multivariate regression analysis showing the contributions of wind and ocean current to ice floe motion.

Parameter	Standardized coeff.	Statistical significance	Pearson corr. coeff.	Partial corr. coeff.	VIF
Intercept		<0.001			
Wind speed	0.729	<0.001	0.766	0.753	1.053
Current speed	0.165	<0.001	0.328	0.251	1.053

Case study 2: An ice floe moving in the drifted ice regime in the Robeson Channel

Figure 11 shows a sequence of daily Sentinel-1 images from 14 to 19 November, where many ice floes originating from the north of the Robeson Channel can be seen. The path of the ice floe marked with the asterisk (floe #29) is linked to the coinc ident wind vectors in Fig. 12. This ice floe moved southward at a speed of 27.0 km d^{-1} between 14 and 15 November. During this period, the wind speed was between 5 and 20 km h^{-1}, with a wide range of directions, but the strongest wind blew from the south to the northeast (Fig. 12). Apparently, this drift was more influenced by the north–south current in this case (daily current maps are not shown). The momentum of the incoming ice floes from the north is a possible explanation for this southward motion. Between 15 and 16 November, relatively strong wind with a speed between 20 and 37 km h^{-1} blew from the south. However, the entire set of floes appear to have drifted eastward. Once again, the wind did not trigger this motion. SSH can be a possible cause because it has a gradient that matches the drift direction (Fig. 7). Between 16 and 18 November, the same strong wind, which approached 30 km h^{-1}, continued to blow to the northeast (Fig. 12), and the entire set of floes responded by drifting in the same direction. Floe #29 reached its highest speed of 11.77 km d^{-1} on 17 November. Between 18 and 19 November, the wind diminished, but a group of ice floes appeared to swirl clockwise. The current continued to be southward, and there was 100% local ice concentration around floe #29.

Commented [57]: Reviewer 1: Wekerle et al. (2013) mentioned that the SSH difference between the Arctic Ocean and Baffin Bay. Detailed information can be found in Response Letter.

Commented [58]: To Reviewer 1: Instead of "continues".

Commented [59]: To Reviewer 1: The sentence is rewritten for better expression.

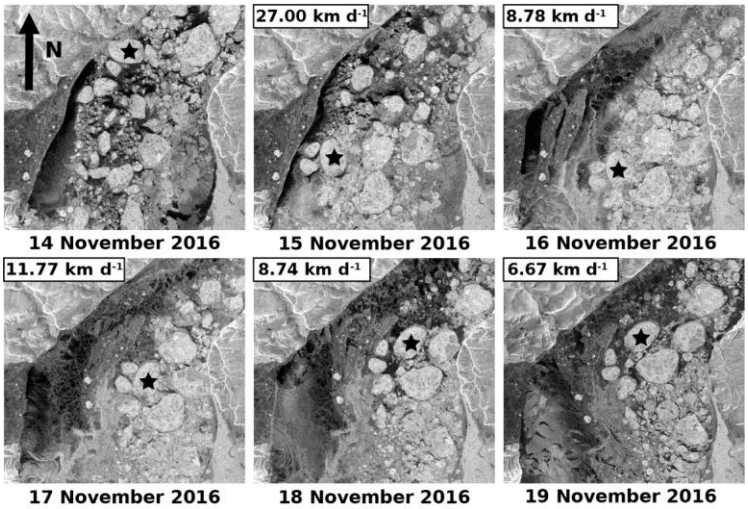

425 **Figure 11**. A sequence of daily Sentinel-1 images showing the path of a number of ice floes. The floe marked by the asterisk (floe #29) is the subject of the comments in the text. Dates of the images are shown, as well as the speed of the marked floe.

Commented [60]: Since the previous Figure 11 was deleted, the subsequent ones have been renumbered.

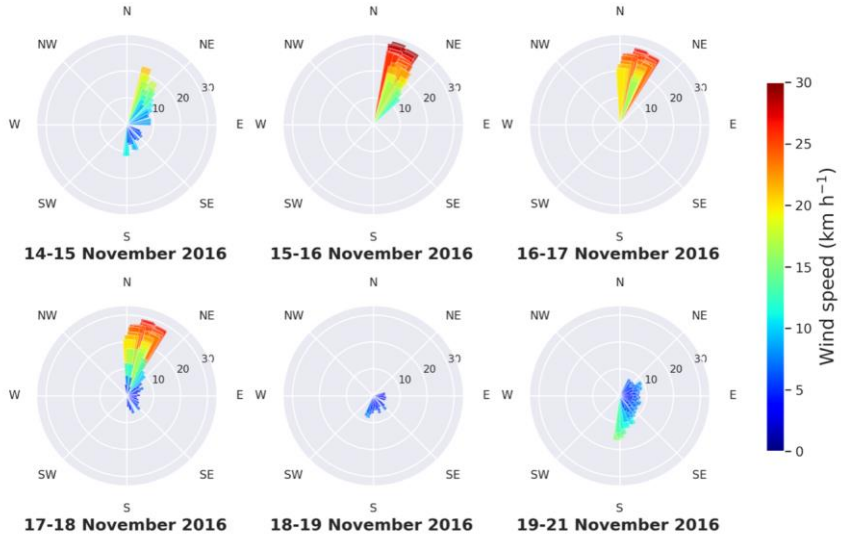

Figure 12. Maps of the 10-m level wind vectors (km h^{-1}) from the ERA5 reanalysis. Each panel has vectors from the four grid points surrounding the location of ice floe #29 every 3 hours during the time between the daily overpasses of Sentinel-1. For example, the 14–15 November panel has the 3-hour vectors between the acquisition times of 14 and 15 November.

Case study 3: An ice floe drifting in the polynya within the Robeson Channel

Fig. 13 shows the track of ice floe #38, which broke off from landfast ice at the Greenland side and drifted north then south in the polynya regime. The trajectory covers the period from 8 to 22 February 2017, after the arch formed. The daily wind vector maps associated with the selected floe location are presented in Fig. 14. Between 10 and 11 February, northward wind dominated, although this never exceeded 20 km h^{-1}. The ice floe drift of nearly 12 km d^{-1} matched the wind direction. Between 13 and 17 February, the northward wind accelerated, reaching 40 km h^{-1} and then 50 km h^{-1}. The ice floe moved in the same direction, with its speed reaching 11.8 km d^{-1}, 32.2 km d^{-1} and 20.4 km d^{-1} on 15, 16 and 17 February, respectively. The speed was significantly reduced to 3.7 km d^{-1} on 18 February as the floe approached the ice arch. After this day, the wind blew from the north and the ice floe changed its direction of motion to advancing southward. It is interesting to note the high ice floe speed of 43.0 km d^{-1} between 20 and 21 February and the highest speed of 99.1 km d^{-1} between 21 and 22 February. The latter was triggered by the highest wind encountered in this study, which gusted to 50 km h^{-1}. However, it is important to recall that

the surface current drives ice motion in the same direction. This case study demonstrates that the influence of the wind on ice motion is the greatest in areas of thin ice and water.

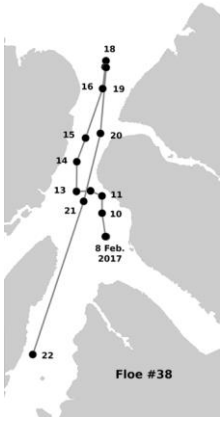

Figure 13. Trajectory of an ice floe (floe #38) that separated from landfast ice and drifted in the polynya regime downstream of the ice arc. The track is shown from 8 to 22 February 2017.

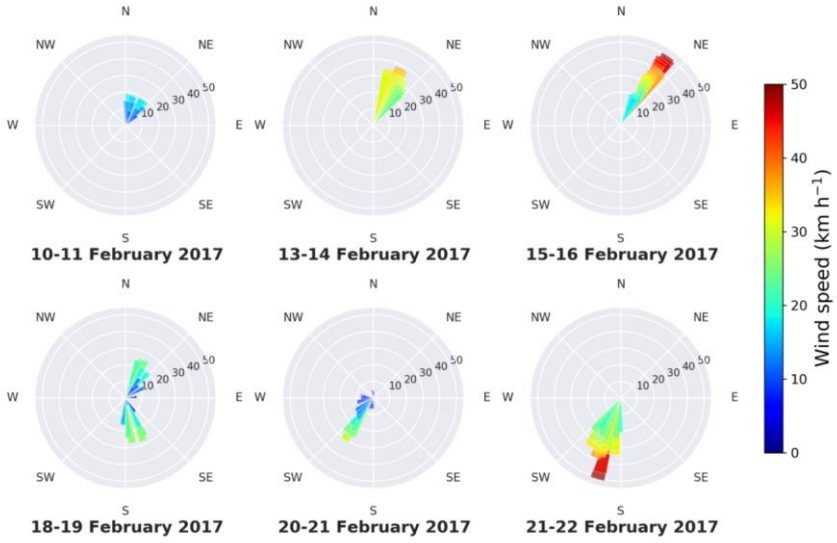

Figure 14. Maps of the 10-m level wind (km h^{-1}), as shown in Fig. 12, but for ice floe #38, which was separated from landfast ice and drifted in the polynya downstream from the ice arch formed at the inlet of the Robeson Channel.

4.2 Formation of the ice arch

The ice arch phenomenon is a necessary condition for polynya formation downstream. Polynyas can be driven by wind action that removes newly formed ice (latent heat polynya), and/or warm upwelling ocean water that melts the ice as soon as it is forms (sensible heat polynya) (Smith et al., 1990). However, if the flux of ice from a nearby source continues to feed into the area that would become a polynya, then the polynya can only be formed if a natural obstacle develops to block the flux. This obstacle could be an ice arch, which is a mechanically strong formation that can withstand the massive dynamic load of the advected sea ice. Clearly, this factor is irrelevant to coastal polynyas as they are backed by land. This is more common in the Antarctic region (Nihashi et al, 2015). In the case of the Robeson Channel, an ice arch commonly forms at the inlet of the channel, blocking the ice flux from the Lincoln Sea into the Robeson Channel. The ice arch may collapse a few weeks after formation or persist as late as mid-August (Samelson et al., 2006). More historical context about the ice arches that form at the inlet of the Robeson Channel can be found in Kwok et al. (2010), Ryan and Münchow (2017) and Moore and McNeil (2018). The ice arch observed in the present dataset started its development on 24 January, matured on 1 February and collapsed in

Commented [61]: To Reviewer 1: Instead of "Polynya". "It is well known that" is also deleted.

Commented [62]: To Reviewer 1: This paper is added as the reference for Antarctic polynya statement.

Commented [63]: To Reviewer 1: Three papers on the context of this ice arch are listed here for readers.

May 2017. The mechanism of arch development is described below. After its initial formation, chunks of ice continued to detach from the arch's contour under the action of the southward wind. This altered the arch's shape and the location of its terminal points along the two constriction points at the Greenland and Ellesmere Island sides. The sequence of the development is revealed in the set of Sentinel-1 images shown in Fig. 15.

The white dashed line that appears in some panels represents the arch's contour of the following day. For example, the dashed line in the image for 24 January represents the arch's contour that appears in the image for 25 January, and so on. No line is presented if the contour remained unchanged in the following day (e.g. the cases of 25 and 26 January). The difference between the visible arch and the dotted line in the image of any given day identifies the ice that was detached by the wind action on that day. The 3-hour wind vectors during the period between the two daily overpasses of Sentinel-1, obtained from the ERA5 reanalysis, are presented in Fig. 16. Data were obtained from the grid points located on lines 3, 4 and 5 in Fig. 3, and are shown in the same colour as that figure.

After seven days of persistent northward wind, southeastward wind returned for a few hours between 22 and 23 January. A wide rupture of ice cover, not forming an arch shape, can be observed in the 23 January image (Fig. 15). Between 23 and 24 January, the dominant southward wind (about 30 km h^{-1}) was strong enough to cause many cracks in the ice cover and introduced the first visible contour of the arch on 24 January. On 25 January, the cracked ice drifted southward and another piece of ice was detached from the arch. On that day, light northward wind occurred (<20 km h^{-1}), but varied over the entire angular range. The same wind prevailed until 28 January, and no change in the arch was observed. When the strong southward wind, reaching 30 km h^{-1}, prevailed from 29 January until 1 February, it first caused numerous cracks to appear on 29 January. The cracked ice was then pushed further south, leaving a well-defined arch shape, as can be seen in the image for 30 January. A major displacement of the arch's end point at the Ellesmere Island side (13.88 km) can be observed. The arch shape continued to be adjusted on 31 January and 1 February, in response to the same strong southward wind. Note the two large pieces of ice that detached in these two days (Fig. 15). After 1 February, the arch remained unchanged, regardless of the wind speed and direction, until it collapsed on 11 May. The only exception was the breakup of a large piece, defined as floe #39, on 5 March (Fig. 17). This piece broke off while the wind was dominantly northward (between 15 km h^{-1} and 30 km h^{-1}). This is not consistent with the aforementioned scenario of the modulation of the arch shape under the action of southward wind. However, it should be noted that the rest of the ice cover in the image for 5 March in Fig. 17 appears to shift north following the northward wind, as indicated by the arrow.

The arch legs, which is an engineering term that refers to the end parts of the arch, can be observed to be perpendicular to the land contour (see the images for 1 and 2 February in Fig. 15). As all the forces exerted on the arch's contour are transferred as compression forces, the arch legs must be perpendicular to the surface, in order to provide a robust way to transfer the load directly to the rock base at both sides. Otherwise, the end point of the arch may continue to slip at the surface, leading to eventual failure of the arch (Karnovsky, 2012). This feature, along with the curvature of the arch, will be of interest to the ice mechanics community.

Figure 15. Daily Sentinel-1 images showing the development of the arch formation from 24 January 2017 until it matured on 2 February 2017. The dotted line marks the arch shape and location in the following day.

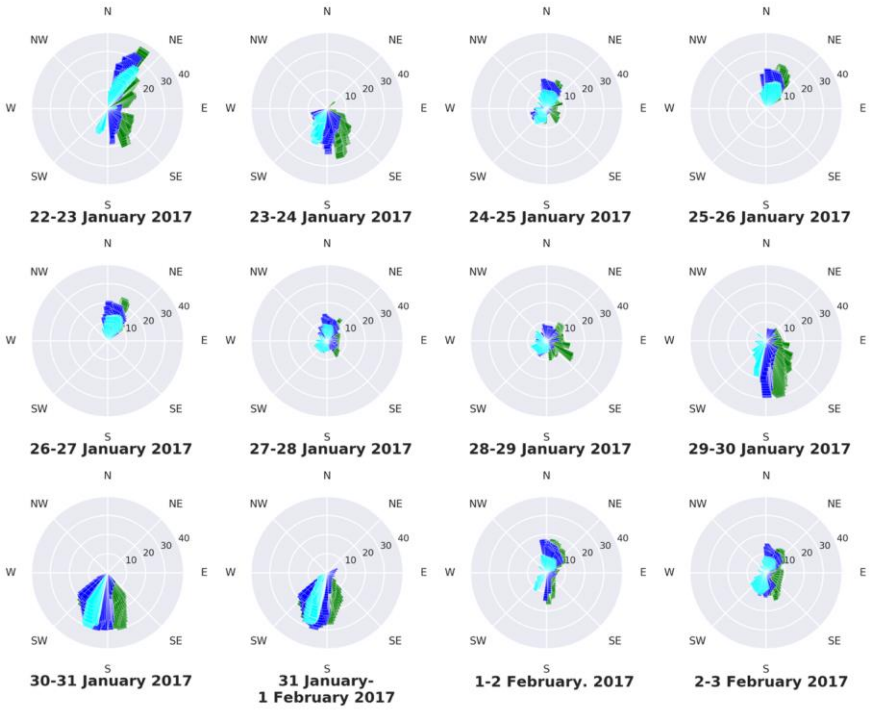

Figure 16. Wind speed (km h^{-1}) during the formation period of the ice arch (22 January to 3 February, 2017), obtained from grid points on lines 3, 4 and 5 (corresponding to latitudes 82.5° N, 82.25° N and 82° N, respectively) of the ERA5 reanalysis shown in Fig. 3. The colours of the vectors are the same as those of the grid points in Fig. 3.

Figure 17. Sequential Sentinel-1 images showing the breakup and drift of an ice piece that was labelled floe #39 in this study. This modulated the ice arch. The arrow indicates the dominant wind direction between the acquisition times of the images for 4 and 5 March.

The above discussion highlights the mechanism of ice arch formation. To reiterate, strong southward wind plays an important role in modulating the arch's contour as it may cause detachment of pieces of ice at the locations of fractures. Northward wind, on the other hand, has virtually no effect on the arch's shape and location. On two occasions, ice pieces were observed to detach in the presence of a light northward wind, which suggests the possible influence of the sea surface current. The modulation of the arch's shape abates when the upstream ice becomes too compacted to allow crack formation, and hence further detachment of ice pieces occurs in response to a southward wind. Moreover, the mechanically strong structure of the arch cannot fail under the dynamic force of the incoming ice flux. The structural properties of the arch were not addressed in this study, except for the observed configuration of its terminal points (arch legs) being perpendicular to the land surface.

Commented [64]: To Reviewer 1: Instead of "chopping".

Commented [65]: To Reviewer 2: Instead of "occasion".

5 Conclusions and recommendations

In this study, a series of daily Sentinel-1A/1B images were used to study the sea ice motion at the scale of individual ice floes in the Robeson Channel, which is located between Greenland and Ellesmere Island, and the process of ice arch formation at the northern entry of the channel. The study period spanned the fall and winter seasons of 2016/2017. Wind data from the ERA5 reanalysis were used to explore the role of wind on ice floe drift and the arch formation process. Daily gridded data of ocean current were also used. In total, 39 floes were visually tracked in the sequential daily images and their velocity vectors were calculated. Qualitative and statistical data of the ice drift were obtained in two regimes, upstream and within the Robeson Channel. Case studies showing links between the drift of selected ice floes and their driving forces were presented. The local reanalysis wind was obtained from the closest grid points to the ice floe at each location on its trajectory.

Sea ice that approaches the Robeson Channel follows a path around the northern section of Ellesmere Island. No ice drift was observed along the coast of Greenland in this case. In the convergent zone that leads to the channel, ice floes drift at a fairly constant speed of around 5 km d^{-1} along erratic paths. This motion seems to be mostly affected by the internal stresses between ice floes in such close pack ice (concentration >70%), with no influence of wind. Wind appears to influence the motion only if the floe is surrounded by thin ice or open water. In this case, a drift speed of up to 18 km d^{-1} was calculated.

Once an ice floe crosses the entry to the channel and becomes released from the stresses engendered by the surrounding ice, it starts to accelerate. While inside the channel, the ice floe drift speed varies between 15 km d^{-1} and 45 km d^{-1}. The direction of motion can be be explained by the combination of wind and ocean currents. A single linear regression analysis between the wind and drift components along the extent of the channel revealed the increasing influence of the wind on ice floe motion when the surrounding ice cover features thin sheet and water. A multivariate regression analysis confirmed that the wind speed

and ocean current speed can explain 72.9% and 16.5% of the ice floe speed, respectively. Available tidal data obtained from the deployed buoys prior to the study period were examined, but no conclusive impact of tide on ice floe motion was found from generating and examining the Fourier spectra of the data.

Commented [66]: Results from linear regression are added.

Ice arch formation and development was monitored using the daily Sentinel-1 images over a 9-day period from 24 January to 1 February 2017. During this period, pieces of ice along the arch's contour continued to crack and detached under the action of southward wind. Northward wind had no role on this process as it closed and tended to stabilize the arch. The process continued until the pack ice upstream of the arch became fully consolidated and the arch took on a mechanically strong concave shape.

Commented [67]: To Review 2: Instead of "dome".

The findings of this study will provide clues to enhance the dynamic modelling of ice by identifying conditions that accentuate the role of wind on ice motion. The study has also demonstrated the possibility of generating non-gridded drift vectors of individual sea ice floes by tracking their motion in a sequenc3 of daily SAR images. Such a product would be important for operational ice mapping as it can identify the distribution of hazardous floes. Daily SAR images covering a limited number of geographic regions have become available from the Sentinel-1 system. They may soon be available from the recently launched RADARSAT Constellation Mission (RCM) (a fleet of three satellites) but only upon request. More SAR constellation systems are expected in the future from several national and commercial agencies. The challenge of generating maps of ice floe drift for sequential SAR images resides in developing an automated identification method for ice floe contours, considering their deformation, rotation, breakup and amalgamation while drifting.

Data availability. Sentinel-1 data are available free of charge from the Copernicus Open Access Hub (https://scihub.copernicus.eu/dhus/#/home, European Space Agency (last accessed: 2 January 2020)). All the reanalysis data are publicly available. The ERA5 hourly data are available from https://cds.climate.copernicus.eu/cdsapp#!/dataset/reanalysis-era5-single-levels?tab=overview (last accessed: 20 December 2019), the ERA-Interim data are available from https://apps.ecmwf.int/datasets/data/interim-full-daily/levtype=sfc/ (last accessed: 13 May 2019), the NCEP/NCAR data are available from https://www.esrl.noaa.gov/psd/data/gridded/data.ncep.reanalysis.html (last accessed: 13 May 2019), the NCEP/DOE data are available from https://www.esrl.noaa.gov/psd/data/gridded/data.ncep.reanalysis2.html (last accessed: 13 May 2019) and the GLORYS12V1 data are available from from http://marine.copernicus.eu/services-portfolio/access-to-products/?option=com_csw&view=details&product_id=GLOBAL_REANALYSIS_PHY_001_030 (last accessed: 12

December 2019). The Alert Station data can be obtained from: https://climate.weather.gc.ca/historical_data/search_historic_data_e.html (last accessed: 5 May 2019).

Author contribution. MES prepared the manuscript, designed the experiments and performed the data analysis. ZHW collected and processed the data. TTL contributed to the data analysis and supported the writing and editing.

Competing interests. The authors declare that they have no conflict of interest.

Acknowledgment. We are grateful to the following organizations for providing the data used in this study. The European Space Agency (ESA) provided the Copernicus Sentinel-1A/1B product. The EMCWF provided the ERA5 and ERA-Interim reanalysis products. The NCEP, NCAR and DOE provided their respective reanalysis products. The CMEMS provided their GLORYS12V1 reanalysis product. The authors would also like to thank the two anonymous reviewers, whose comments have improved the manuscript greatly.

Financial support. This work was supported in part by the National Key Research and Development Program of China (2018YFC1406102), the fund of the Key Laboratory of Global Change and Marine-Atmospheric Chemistry (GCMAC1806), and the National Natural Science Foundation of China (41676179 and 41941010).

References

Bourbigot, M., Johnsen, H., Piantanida, R., and Hajduch, G.: Sentinel-1 product definition, MDA, SEN-RS-52-7440, 2016.

Copernicus Climate Change Service (C3S): ERA5: Fifth generation of ECMWF atmospheric reanalyses of the global climate, Copernicus Climate Change Service Climate Data Store (CDS), https://doi.org/10.24381/cds.adbb2d47, 2017.

Dee, D. P., Uppala, S. M., Simmons, A. J., Berrisford, P., Poli, P., Kobayashi, S., Andrae, U., Balmaseda, M. A., Balsamo, G., Bauer, P., Bechtold, P., Beljaars, A. C. M., Berg, L. van de, Bidlot, J., Bormann, N., Delsol, C., Dragani, R., Fuentes, M., Geer, A. J., Haimberger, L., Healy, S. B., Hersbach, H., Hólm, E. V., Isaksen, L., Kållberg, P., Köhler, M., Matricardi, M., McNally, A. P., Monge-Sanz, B. M., Morcrette, J.-J., Park, B.-K., Peubey, C., Rosany, P. de, Tavolato, C., Thépaut, J.-N., and Vitart, F.: The ERA-Interim reanalysis: configuration and performance of the data assimilation system, Q. J. Roy. Meteor. Soc., 137, 553–597, https://doi.org/10.1002/qj.828, 2011.

Demchev, D., Volkov, V., Kazakov, E., Alcantarilla, P. F., Sandven, S., and Khmeleva, V.: Sea ice drift tracking from Sequential SAR images using accelerated-KAZE features, IEEE T. Geosci. Remote, 55(9), 5174–5184, https://doi.org/10.1109/TGRS.2017.2703084, 2017.

Dumont, D., Gratton, Y., and Arbetter, T. E.: Modelling the dynamics of the North Water Polynya ice bridge, J. Phys. Oceanogr., 39(6), 1448–1461, https://doi.org/10.1175/2008JPO3965.1, 2009.

Fernandez, E. and Lellouche, J. M.: Product user manual for the Global Ocean Physical Reanalysis Product GLORYS12V1, Copernicus Product User Manual, 4, 1–15, 2018.

Gimbert, F., Marsan, D., Weiss, J., Jourdain, N. C., and Barnier, B.: Sea ice inertial oscillations in the Arctic Basin, Cryosphere, 6, 1187–1201, https://doi.org//10.5194/tc-6-1187-2012, 2012.

Godin, G.: Currents in Robeson Channel, Nares Strait, Mar. Geod., 2(4), 351–364, https://doi.org/10.1080/15210607909379362, 1979.

Gudmandsen, P.: A remote sensing study of Lincoln Sea, in: Proceeding of the ERS-ENVISAT Symposium, Gothenburg, Sweden, 16–20 October, 461, 2084–2090, 2000.

Hall, R. T. and Rothrock, D. A.: Sea ice displacement from Seasat Synthetic Aperture Radar, J. Geophys. Res.-Ocean, 86(NC11), 1078–1082, https://doi.org/10.1029/JC086iC11p11078, 1981.

Herlinveaux, R. H.: Oceanographic observations in Robeson Channel, N.W.T., Pacific Marine Science Report 79–16, Institute of Ocean Science, Patricia Bay, Sidney, B.C., Canada., 1971.

Johnson, H. L., Münchow, A., Falkner, K. K., and Melling, H.: Ocean circulation and properties in Petermann Fjord, Greenland, J. Geophys. Res., 116, C01003, https://doi.org/10.1029/2010JC006519, 2011.

Kalnay, E., Kanamitsu, M., Kistler, R., Collins, W., Deaven, D., Gandin, L., Iredell, M., Saha, S., White, G., Woollen, J., Zhu, Y., Chelliah, M., Ebisuzaki, W., Higgins, W., Janowiak, J., Mo K. C., Ropelewski, C., Wang, J., Leetmaa, A., Reynolds, R., Jenne, R., and Dennis, J.: The NCEP/NCAR 40-year reanalysis project, Bull. Amer. Meteor. Soc., 77, 437–470, https://doi.org/10.1175/1520-0477(1996)077<0437:TNYRP>2.0.CO;2, 1996.

Kanamitsu, M., Ebisuzaki, W., Woollen, J., Yang, S.-K., Hnilo, J. J., Fiorino, M., and Potter, G. L.: NCEP-DOE AMIP-II Reanalysis (R-2), Bull. Amer. Meteor. Soc., 83(11), 1631–1644, https://doi.org/10.1175/bams-83-11-1631, 2002.

Karnovsky, I. A.: Theory of arched structures: strength, stability and vibration, Springer, New York Dordrecht Heidelberg London, ISBN: 978-1-4614-0468-2, 423p, https://doi.org/10.1007/978-1-4614-0469-9, 2012.

Commented [68]: New reference

Commented [69]: New reference

Kimura, N. and Wakatsuchi, M.: Relationship between sea-ice motion and geostrophic wind in the Northern Hemisphere, Geophys. Res. Lett., 27(22), 3735–3738, https://doi.org/10.1029/2000GL011495, 2000.

Kwok, R.: Variability of Nares Strait ice flux, Geophys. Res. Lett., 32(24), L24502, https://doi.org/10.1029/2005GL024768, 2005.

Kwok, R. and Cunningham, G. F.: Seasonal ice area and volume production of the Arctic Ocean: November 1996 through April 1997, J. Geophys. Res.-Ocean, 107 (C10), 8038, https://doi.org/10.1029/2000JC000469, 2002.

Kwok, R., Spreen, G., and Pang, S.: Arctic sea ice circulation and drift speed: Decadal trends and ocean currents, J. Geophys. Res. Oceans, 118, 2408–2425, https://doi:10.1002/jgrc.20191, 2013.

Kwok, R., Toudal-Pederson, L., Gudmandsen, P., and Pang, S.: Large sea ice outflow into Nares Strait in 2007, Geophys. Res. Lett., 37, L03502, https://doi.org/10.1029/2009GL041872, 2010.

Leberl, F., Raggam, J., Elachi, C., and Campbell, W. J.: Sea ice motion measurements from SEASAT SAR images, J. Geophys. Res.-Ocean, 88(NC3), 1915–1928, https://doi.org/10.1029/JC088iC03p01915, 1983.

Lellouche, J. M., Greiner, E., Le Galloudec, O., Garric, G., Regnier, C., Drevillon, M., Benkiran, M., Testut, C. E., Bourdalle-Badie, R., Gasparin, F., Hernandez, O., Levier, B., Drillet, Y., Remy, E., and Le Traon, P. Y.: Recent updates on the Copernicus Marine Service global ocean monitoring and forecasting real-time 1/12° high resolution system, Ocean Sci., 14, 1093–1126, https://doi.org/10.5194/os-2018-15, 2018.

Leppäranta, M.: The drift of sea ice, Springer Science & Business Media, ISBN-10: 3540408819, https://doi.org/10.1007/978-3-642-04683-4, 2011.

McNutt, S. L. and Overland, J. E.: Spatial hierarchy in Arctic sea ice dynamics, Tellus A., 55(2), 181–191, https://doi.org/10.1034/j.1600-0870.2003.00012.x, 2003.

Moore, G. W. K and McNeil, K.: The early collapse of the 2017 Lincoln Sea ice arch in response to atmospheric sea ice and wind forcing, Geophys. Res. Lett., 45 (16), 8343–8351, https://doi.org/10.1029/2018GL078428, 2018.

Münchow, A. and Melling, H.: Ocean current observations from Nares Strait to the west of Greenland: Interannual to tidal variability and forcing, J. Mar. Res., 66(6): 801-833, https://doi.org/10.1357/002224008788064612, 2008.

Münchow, A., Falkner, K. K., and Melling, H.: Spatial continuity of measured seawater and tracer fluxes through Nares Strait, a dynamically wide channel bordering the Canadian Archipelago, J. Mar. Res., 65(6): 759-788, https://doi.org/10.1357/002224007784219048, 2007.

Commented [70]: New reference

Nihashi, S. and Ohshima, K. I.: Circumpolar map of Antarctica coastal polynya and landfast sea ice: relationship and variability, J. Climate, 28 (9), 3650-3670, https://doi.org/10.1175/JCLI-D-14-00369.1, 2015.

Ryan P. A. and Münchow, A.: Sea ice draft observations in Nares Strait from 2003 to 2012, Journal of Geophy. Res., Ocean, 122, 3057–3080. https://doi.org/10.1002/2016JC011966, 2017.

Rasmussen, T. A. S., Kliem, N., and Kaas, E.: Modelling the sea ice in the Nares Strait, Ocean Model., 35(3), 161–172, https://doi.org/10.1016/j.ocemod.2010.07.003, 2010.

Samelson, R. M., Agnew, T., Melling, H., and Münchow, A.: Evidence of atmospheric control of sea-ice motion through Nares Strait, Geophys. Res. Lett., 33(2), L02506, https://doi.org/10.1029/2005GL025016, 2006.

Shroyer, E. L., Samelson, R. M., Padman, L., and Munchow, A.: Modeled ocean circulation in Nares Strait and its dependence on landfast-ice cover, J. Geophys. Res.-Oceans, 120, 7934–7959, https://doi.org/10.1002/2015JC011091, 2015.

Smith, S. D., Muench, R. D., and Pease, C. H.: Polynyas and leads: An overview of physical processes and environment, J. Geophys. Res.-Ocean, 95(C6), 9461–9479, https://doi.org/10.1029/JC095iC06p09461, 1990.

Tang, C. L., Ross, C. K., Yao, T., Petrie, B., DeTracey, B. M., and Dunlap, E.: The circulation, water masses and sea-ice of Baffin Bay, Prog. Oceanogr., 63(4), 183–228, https://doi.org/10.1016/j.pocean.2004.09.005, 2004.

Thorndike, A. S. and Colony, R.: Sea ice motion in response to geostrophic winds, J. Geophys. Res.-Ocean, 87(C8), 5845–5852, https://doi.org/10.1029/JC087iC08p05845, 1982.

Vincent, R. F., Mardsen, R. F., and McDonald, A.: Short time-span ice tracking using sequential AVHRR imagery, Atmosphere-Ocean, 39 (3), 279-288, http://doi/10.1080/07055900.2001.9649681, 2001.

Wekerle, C., Wang, Q., Danilov, S., Jung, T., and Schröter, J.: The Canadian Arctic Archipelago throughflow in a multiresolution global model: Model assessment and the driving mechanism of interannual variability, J. Geophys. Res. Oceans, 118, 4525–4541, https://doi.org/10.1002/jgrc.20330, 2013.

Commented [71]: New reference

Commented [72]: New reference